HEURISTIC APPROACHES FOR THE MULTI-OBJECTIVE ROUTING PROBLEM FOR A FLEET OF UNMANNED AERIAL VEHICLES

İNSANSIZ HAVA ARACI FİLOSUNUN ÇOK-AMAÇLI ROTALAMA PROBLEMİ İÇİN SEZGİSEL YAKLAŞIMLAR

BÜŞRA BİŞKİN

ASST. PROF. DR. DİCLEHAN TEZCANER ÖZTÜRK

Supervisor

ASST. PROF. DR. CEREN TUNCER ŞAKAR

Co-Supervisor

Submitted to

Graduate School of Engineering of Hacettepe University

as a Partial Fulfillment to the Requirements

for the Award of the Degree of Master of Science

in Industrial Engineering.

2019

ÖZET

İNSANSIZ HAVA ARACI FİLOSUNUN ÇOK-AMAÇLI ROTALAMA PROBLEMİ İÇİN SEZGİSEL YAKLAŞIMLAR

Büşra BİŞKİN

Yüksek Lisans, Endüstri Mühendisliği Bölümü

Tez Danışmanı: Dr. Öğr. Üyesi Diclehan TEZCANER ÖZTÜRK

Eş Danışman: Dr. Öğr. Üyesi Ceren TUNCER ŞAKAR

Aralık 2019, 64 sayfa

Günümüzde, İnsansız Hava Araçları (İHA'lar), farklı amaçlarla çeşitli görevlerde yaygın olarak kullanılmaktadır. Her görevde, farklı amaçlar ve problem yapıları göz önünde bulundurulmaktadır. Bu tezde, özdeş İHA'lardan oluşan bir İHA filosunun rotalama problemi, birden fazla amaç gözetilerek incelenmiştir. Filodaki İHA'lar, sahip oldukları sınırlı uçuş süreleri içerisinde ve iki boyutlu bir görev alanında hareket etmek üzere, bir üsten ayrılır, belirli bir sayıdaki hedefi ziyaret eder ve üsse geri dönerler. Hedeflerin farklı öncelikleri olduğu varsayılmakta olup İHA'ların maksimum seviyede ödül toplamak için uçuş limitleri dahilinde mümkün olduğu kadar çok hedefi ziyaret etmeye çalışması beklenir. Bu çalışmadaki rotalama probleminde göz önünde bulundurulan üç amaç: filonun kat ettiği toplam mesafeyi en aza indirgemek, hedeflerden toplanan toplam ödülü en üst seviyeye çıkarmak ve toplam radar tehdidini en aza indirmektir. Rotalama

probleminin iki versiyonu ele alınmıştır. Bu versiyonlar: radarsız bir alanda rotalama (amaç olarak mesafe ve ödül gözetilerek) ve radarla izlenen bir arazide rotalamadır (her üç amaç da gözetilerek). Filodaki her İHA için etkin bir rota ve her rotadaki hedef çiftleri arasında etkin yollar bulmak amaçlanmıştır.

Problemin her iki versiyonu için iki çözüm yaklaşımı kullanılmıştır. İlk yaklaşımda, problem Çok Amaçlı Takım Oryantiring Problemi olarak modellenmiş ve kesin çözümler bulunmuştur. İkinci yaklaşımda, makul sürede etkin çözümler üretmek için evrimsel bir algoritma olan EA-fUAV kullanılmıştır. Her iki yaklaşım da üç farklı problem vakasında test edilmiştir. Sonuçlar, EA-fUAV'ın etkin çözüm setine makul bir zamanda yaklaştığını göstermektedir.

Anahtar Kelimeler: Çok-amaçlı Optimizasyon, Evrimsel Algoritma, Çok Amaçlı Takım Oryantiring Problemi, İnsansız Hava Aracı

ABSTRACT

HEURISTIC APPROACHES FOR THE MULTI-OBJECTIVE ROUTING PROBLEM FOR A FLEET OF UNMANNED AERIAL VEHICLES

Büşra BİŞKİN

Master of Science, Department of Industrial Engineering

Supervisor: Asst. Prof. Dr. Diclehan TEZCANER ÖZTÜRK

Co- Supervisor: Asst. Prof. Dr. Ceren TUNCER ŞAKAR

December 2019, 64 pages

Nowadays, Unmanned Aerial Vehicles (UAVs) are extensively employed for various missions with different purposes. In every mission, different goals and problem structures are considered. In this thesis, we study the routing problem of a fleet of identical UAVs under multiple objectives. UAVs in the fleet, which have limited flight durations, take off from a base, visit a number of targets in a two-dimensional mission area, and return to the base. We assume that the targets have different priorities, and the UAVs try to visit as many targets as possible to collect maximum reward within flight limits. We consider the following three objectives: minimizing the total distance traveled by the fleet, maximizing the total reward collected from the targets, and minimizing the total radar threat. We address two versions of the problem: routing in a radar-free terrain (with distance and

reward as objectives) and routing in a radar-monitored terrain (with all three objectives). We aim to find efficient routes for each UAV in the fleet and the trajectory between pairs of targets in each route.

We employ two solution approaches for each version of our problem. First, we model the problem as a Multi-Objective Team Orienteering Problem (MOTOP) and find exact solutions. In our second approach, we utilize an Evolutionary Algorithm, EA-fUAV (Evolutionary Algorithm for routing a fleet of UAVs), to approximate efficient solutions in reasonable time. We test both approaches on three different problem cases. The results show that EA-fUAV approximates the efficient set well in reasonable time.

Keywords: Multi-objective Optimization, Evolutionary Algorithm, Multi-Objective Team Orienteering Problem, Unmanned Aerial Vehicle

ACKNOWLEDGEMENTS

I would like to express my gratitude to my supervisors, Asst. Prof. Dr. Diclehan TEZCANER ÖZTÜRK and Asst. Prof. Dr. Ceren TUNCER ŞAKAR, for their unflagging support, patience, motivation, and immense knowledge. I consider myself very lucky to work with them and never forget our fruitful and amusing discussions. Their reliance on me made this work done, I wish our collaboration lasts years.

I am grateful to my family, my father, my mother and my brother. They always become light on my darkest moments and take care of me in all aspects.

I must thank all my close friends for always being beside me, cheering me up and for their demulcent trust on my work. I also thank my coworkers in Gazi University for sharing their experiences on academic life and assisting me at busy periods.

Finally, I would like to express my gratitude to everyone who directly or indirectly contributed to this work.

Büşra BİŞKİN

December 2019, Ankara

TABLE OF CONTENTS

LIST OF FIGURES

LIST OF TABLES

ABBREVIATIONS

DDD	Dull, Dangerous and Dirty
EA	Evolutionary Algorithm
MILP	Mixed Integer Linear Programming
MOEA	Multi-Objective Evolutionary Algorithm
MOTOP	Multi-Objective Team Orienteering Problem
NN	Nearest Neighborhood
NSGA-II	Non-Dominated Sorting Genetic Algorithm
OP	Orienteering Problem
PCLRP	Prize Collecting Location and Routing Problem
UAV	Unmanned Aerial Vehicle
VNS	Variable Neighborhood Search
VND	Variable Neighborhood Descent
VRP	Vehicle Routing Problem

1. INTRODUCTION

Unmanned Aerial Vehicles (UAVs) are aircrafts that do not require an attendant human pilot and commonly, they are either remote-controlled or programmed to fly autonomously (Valavanis and Vachtsevanos, 2015). With the development of technology and requirements, utilization variety of UAVs for tasks and objectives has increased. Austin (2010) argue that the role of UAVs has gone far beyond the military proverb DDD (dull, dangerous and dirty) tasks. Unmanned Aerial Vehicles can attain areas where it is risky or impossible for humans to survive in terms of flight capabilities such as range, stamina, and altitude.

Korkmaz et al. (2015) claim that modern UAVs date back to the last twenty years and classify UAVs into two as military and civilian. UAVs can be employed to track the atmosphere in civil applications (for collecting data such as temperature, humidity), traffic interflow and disaster relief activities, thus increasing the speed and probability of knowledge collection and interference in civilians. In military applications, UAVs can perform very difficult and life-threatening tasks for manned aircrafts as reconnaissance missions, espionage, detecting and attacking targets, or even frontline search and rescue operations. Especially for reconnaissance missions, long flight times, flexible positioning close to possible targets and the relative difficulty of being detected due to their small size and flying capability as a fleet are some of the reasons why UAVs are preferred.

UAVs are used for several missions, and at each mission, different objectives and problem structures should be considered. In reconnaissance missions, UAVs need to visit specific target locations and monitor large terrains for data gathering. Additionally, exposure of UAVs to enemy threats like radars are considered as an important risk factor. In military and civilian operations, minimizing distance traveled, the number of UAVs used, travel time, fuel consumption, detection threat, and maximizing the number of targets visited are widely used objectives in the literature. The routes that the UAVs follow are structured considering a subset of these objectives.

In general, the objectives conflict with each other, making the task of finding routes complicated. For example, in order to reduce detection by threats, UAV can avoid directly flying over the threats that may result in an increase in the length and the duration of the travel. Since the fuel availability limits the flight of the UAV, there may be cases where the UAV cannot visit all targets. For such cases, selection among targets and/or prioritization of targets might be necessary.

In this study, we aim to find routes for a fleet of homogenous Unmanned Aerial Vehicles. The UAVs start with a common base, visit multiple targets and turn back to the base in a two-dimensional area. Each UAV can travel a limited distance since there is an endurance limit on UAVs and thus they visit a subset of the targets, which are prioritized relatively. We structure the routes considering three objectives; minimization of the total distance traveled, minimization of the radar detection threat, and maximization of the total reward (priority) collected from the targets visited. The problem is modeled as a Mixed Integer Linear Program (MILP) considering that the problem is NP-Hard and requires too much time to solve, a heuristic method based on NSGA-II is utilized for solving the problem.

In Section 2 of this study, related literature on UAV routing is reviewed. In Section 3, the UAV routing problem studied in this thesis is explained. Section 4 covers the methodology developed to solve this problem. In Section 5, three different applications for the problem are demonstrated and the results of computational studies are given. In Section 6, conclusions are presented.

2. LITERATURE REVIEW

In the last decade, the UAV routing problem has attracted much attention from researchers. Since, UAV is a development that improves processes and eliminates the life-threatening danger in military and civilian fields. Thereby, usage of UAVs increased in daily life. The literature on UAV routing shows a variety of approaches. Coutinho et al. (2018) present the increase in the number of published papers in UAV path planning between 1998 and 2016. This study includes literature statistics gained from 70 UAV routing/trajectory optimization/path planning/task assigning papers published between 2010 and 2016. According to these statistics, 51.4% of papers deal with a fleet of UAVs and in 28.6% of the papers, UAVs are considered as capacitated. In 71.4% of the papers, multiple waypoints must be visited and in 54.3% of the studies visiting order of waypoints is obscure.

As indicated, almost half of the literature is on routing one single UAV. A single UAV routing issue where there are several depots are taken into consideration in the study of Sundar and Rathinam (2014), and the vehicle can be refilled in all depots. The purpose of the problem is to find the UAV route to ensure that each target is visited by the vehicle at least once. The problem is modeled by using MILP and solved by an approximation algorithm. Ousingsawat (2006) aims to maximize the coverage of the target area with different priorities in the shortest time considering velocity and turning radius as constraints. The target area is divided into equal rectangular parts and priorities are defined by assigning entropy on each part; the summation of these entropies is taken as coverage. Entropy is considered as the uncertainty of the area and higher entropy means higher priority. The area is covered using the model of lawn-mower working progress. A path planning algorithm is developed for the UAV using hybrid modeling in a two-dimensional plane. UAV motion dynamics are restricted as going straight, turning left and turning right for the simplification of the problem. Hernández-Hernández et al. (2014) route a single UAV considering danger zones, time and speed restrictions for 3 different objective functions, minimizing time spent, consumption of fuel and divergence of area. Other multi-objective routing problems of single UAV are studied in Tezcaner and

Köksalan (2011) and Tezcaner Öztürk and Köksalan (2016). In the study, UAV visits all targets and returns to the starting point considering two objective functions. Points which can be reached in the area of movement are predetermined and objective functions minimize overall distance and total threat of radar detection. In this paper, an interactive algorithm has been developed to find the most preferred route for the route planner with a quasi-concave preference function instead of finding all routes. In the second study, an interactive algorithm has been developed to find the most preferred route of a route planner with a quasi-concave preference function. In the study of Tezcaner Öztürk and Köksalan (2018), the UAV can fly to every point in the continuous space. Solution methods are developed to find all the effective routes considering similar objectives and problem structure to the previous studies. Türeci (2017) has developed interactive algorithms that find the route planner's most preferred routes for the UAV that flies in continuous space. The objectives and problem structure used in Tezcaner and Köksalan (2011) and Tezcaner Öztürk (2013) are also used in Türeci (2017).

One of the advantages of UAVs as Korkmaz et al. (2015) claim is that they can fly in teams and move in a coordinated manner so they can scan large areas in a short time. Lamont et al. (2007) aim to design a comprehensive mission planning system by considering UAVs as a swarm. The objectives of the problem are minimizing the cost and risk. In the study of Peng and Gao (2008), the traditional vehicle routing problem with stochastic demand is adapted to the reconnaissance problem with the stochastic observation of multiple UAVs. The problem has multiple objectives of optimizing task period, total time and the number of vehicles required. The problem is solved by using the steady-state multi-objective evolutionary algorithm. Levy et al. (2014) add fuel constraints and fuel stations that can be visited by UAVs during the tour for refueling. In their problem, there are multiple depots and multiple UAVs with fuel constraints. The goal is to find a tour for each UAV, where all specified targets are visited by some UAV at least once. Therefore, it is needed to partition the targets among the UAVs and find a feasible tour for each. The authors also aim to minimize travel cost which is considered as the total fuel consumed by all UAVs and it is assumed as directly proportional to the distance traveled by an UAV. UAVs are heterogeneous, they have different fuel tank capacities. This study focuses on developing heuristics that can find a solution as quick

as possible. Therefore, Variable Neighborhood Search (VNS) and Variable Neighborhood Descent (VND) metaheuristic frameworks are used.

In the paper of Wu et al. (2018), tasks of UAVs are divided into three parts as reconnaissance, combat, and strike. It is assumed that every task has its constraints and UAVs specified for the tasks also have constant flight levels. Targets are taken as known and stationary. Since there are multiple heterogeneous UAVs, the task assignment process was done by using Dubin's path cost. Constraints of the problem were also categorized into three, which are trajectory level, task level, and environment level. Trajectory level includes curvature, heading angle on target and double attack constraints. On the environmental level, there are threat and obstacle avoidance constraints and task level constraints are task precedence restriction, task execution time and limited resources onboard. The objective function of the problem is minimizing a cost function which includes cumulative distance traveled by the UAVs plus maximum length of trajectory for all UAVs involved as constraint. This study uses a distributed genetic algorithm for finding a solution and creates a coupled method including task assignment and trajectory generation.

Karakaya (2014) intends to maximize the covered number of targets with the predefined number of UAVs considering the flight range of them. Flight dynamics are neglected. A modified Max-Min Ant System is proposed to solve the problem and it is compared to the Nearest Neighborhood (NN) algorithm. The proposed method was shown to be more successful. Alotaibi et al. (2018) also considers the presence of threats because military operations being detected or stopped by the enemy have importance. Therefore, in this research, route is planned not only to maximize the number of targets visited, but also to reduce the level of exposure to the threats and travel period. As accepted vulnerability to threats decreases, UAV tries to travel farther away from the threat and this prolongs travel time, and vice versa. A MILP is designed to optimize the total number of targets visited by several UAVs while restricting the travel time as well as the overall threat level. The formula is based on the Vehicle Routing Problem (VRP) with set covering. In the article, waypoints that a UAV can fly from one target to another to reduce the level of risk on high threat levels are created. Multiple UAVs visit multiple targets without limiting the

number or order of targets for a UAV. The problem is solved with a Branch-and-Cut-and-Price methodology with a simple route heuristic.

The study of Yakıcı (2016) can be classified as mission planning for UAVs including location and routing. The goal is to collect awards which can be found in the Orienteering Problem (OP) as a combination of node choice and to find the shortest Hamiltonian route with the chosen nodes. Team Orienteering Problem, which is the generalization of OP, aims to maximize the collected scores. Therefore, this article defines its problem in Team Location and Orienteering Problem and named as "Prize Collecting Location and Routing Problem (PCLRP)". It includes multiple location selection, multiple routing, prize collection, and fixed fleet. The case contains homogeneous UAVs, base stations and fixed interest points which have importance values. The problem involves randomly generated instances of limited flight time on UAVs, and it was solved by a heuristic approach based on Ant Colony Optimization where UAVs are considered as ants.

Regard to the literature review, it is realized that there are no studies on UAV routing that consider the presence of threats, prize collecting and flight limits together. This thesis focuses on routing a fleet of homogenous UAVs while considering flight limits on UAVs and multiple objectives. In the study, the reward is assigned to every predefined target and there are two versions of the routing problem. In the first one, finding a route for each UAV is aimed while maximizing total reward collected from targets and minimizing the total distance traveled by the fleet. In the second version of the problem, another objective is added, minimizing total radar detection threat. Therefore, trajectories between each target need to be defined with the UAV routes. The Problem can be classified as Team Orienteering Problem, which is NP-hard (Chao et al., 1996), and modeled as a Mixed Integer Linear Programming. Exact solutions are found for small-sized problems, and to find solutions quickly for larger problems, a well-known multi-objective evolutionary algorithm, NSGA-II, with adjustments is utilized (Deb et al., 2002).

3. MULTI-OBJECTIVE ROUTING PROBLEM OF A FLEET OF UAVS

In this study, we develop routes for a fleet of identical UAVs. It is assumed that the UAVs make their moves in a two-dimensional area, they depart from a common base, visit some of the predetermined targets within their flight limits, and turn back to the base. Target locations are fixed, targets can only be visited once by one UAV and reward values that imply the relative priorities of the targets are assigned to them. Additionally, the UAVs try to minimize the radar threat.

We aim to maximize the total reward collected from the targets by the UAVs with limited flight distance range while minimizing the total distance traveled by the fleet and the total radar threat the fleet is exposed to. We consider two versions of this problem: two-objective version determines routes in a radar-free terrain, and three-objective version determines routes in a terrain monitored by radars. In the two-objective version, there is a single efficient trajectory between target pairs. Consequently, we answer two questions: "Which targets will be visited by which UAV?" and "In which order these targets will be visited?". In the three-objective case, where there are radars in the terrain, there are countless trajectories linking pair of targets, each trajectory having a better distance or radar detection threat value compared to another. Therefore, a third question to be answered is "Which path will be used between two targets?". In this section, we describe the structure of the problem in detail.

Definitions

Definitions of terms frequently used in this thesis are given here, which are adjusted from the study of Köksalan and Tezcaner Öztürk (2017).

Let x represent the decision vector in X, where X denotes the feasible set. Z denotes the image of the feasible set in objective function space. Assume that p objectives are to be

minimized and $z(x) = \left(z_1(x), z_2(x), \ldots , z_p(x) \right)$ is the objective function vector of *x*, $z_k(x)$ is the solution *x* performance of objective *k*.

Definition 3.1 A solution $x \in X$ is said to be efficient if there is no $x' \in X$ such that $z_k(x') \leq z_k(x)$ for $k = 1, 2, \ldots , p$ and $z_k(x') < z_k(x)$ for at least one objective. Existence of such an x' , makes *x* inefficient. The efficient frontier (set) is the set of all efficient solutions.

Definition 3.2 If a solution $x \in X$ is efficient, then *z(x)* is said to be nondominated, and *z(x)* is said to be dominated when *x* is inefficient. The nondominated frontier (Pareto optimal front) is comprised of the set of all nondominated points.

Assumptions

The following are the assumptions made in this thesis:

Assumption 3.1 The fleet is composed of identical UAVs and they move with constant speed.

Assumption 3.2 Mission area is two-dimensional and the UAVs fly at a constant altitude.

Assumption 3.3 Targets, the base, and radar locations are predefined and stationary. Each target has a predetermined significance value for the mission.

Assumption 3.4 The UAVs do not spend time at the targets.

3.2. Definition of Criteria

There are three criteria considered in this thesis which are total distance traveled by the fleet, total radar detection threat and total reward collected from the targets. We aim to minimize the total distance traveled by the fleet and the total radar detection threat while maximizing the total reward collected from the targets. We next explain the criteria.

3.2.1. Distance

UAVs have specific flight dynamics with regard to their model; this study takes two of them into consideration, maximum flight duration and maximum cruising speed. These two attributes designate a maximum flight distance on UAVs since distance is proportional to speed and time as showed in Equation (3.1). *D*, *S* and *T* stand for distance, speed and time, respectively.

$$D = S \times T \tag{3.1}$$

Therefore, it is assumed that there is a predetermined flight distance limit on each UAV, their total route distance should be within this limit. Furthermore, in missions that require urgency, UAVs should return to the base point as fast as possible, so they either accelerate or travel less distance. It is supposed that UAVs have constant speed, they should travel less distance in order to be quick. This conceives one of the objectives of the problem as minimizing the total distance traveled by the fleet.

Total distance traveled by the fleet is calculated as the sum of the distances of the routes of each UAV in the fleet. When UAVs move in a radar-free terrain, they travel the shortest distance between two targets, that is the Euclidean distance connecting two targets.

Let p_1 and p_2 be two points in a two dimensional area and (x_i, y_i) show the coordinates of point *i* as in Figure 3.1, the Euclidean distance between two points (d) is calculated as in Equation (3.2).

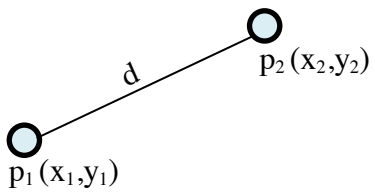

Figure 3.1. Euclidean distance

Euclidean distance (d) = $\sqrt{(x_2 - x_1)^2 + (y_2 - y_1)^2}$ (3.2)

Let *i* and *j* be indices of the target and base set *I* and *u* be the index of the UAV set *U*. In that case, the total distance traveled by the fleet is as in Equation (3.3).

$$d = \sum_{i \in I} \sum_{j \in I} \sum_{u \in U} d_{ij} X_{iju} \tag{3.3}$$

where,

d_{ij}: distance between targets $i \in I$ and $j \in I$

$$X_{iju} = \begin{cases} 1 & if\ UAV\ u\ flies\ from\ target\ i\ to\ target\ j \\ 0 & otherwise \end{cases}$$

In the three-objective version, we assume that the radars are effective in detecting the UAV in a circular area in which the radar is settled at the center of the circle. An example can be seen in Figure 3.2 where we have two targets and a radar in between. In general, if UAVs move in a continuous terrain, there are infinitely many trajectory alternatives between pairs of targets under the conflicting objectives of distance minimization and radar detection threat minimization. To find some of these trajectories between target pairs, we discretize the radar's effective area with equidistant grids and allow the UAVs to move between the grid points while passing through the radar's effective area. This movement is explained in detail in Section 3.3.2. We then calculate the distance of a trajectory as the sum of Euclidean distances between waypoints in and out of the radar area. Two trajectories are shown in Figure 3.2.

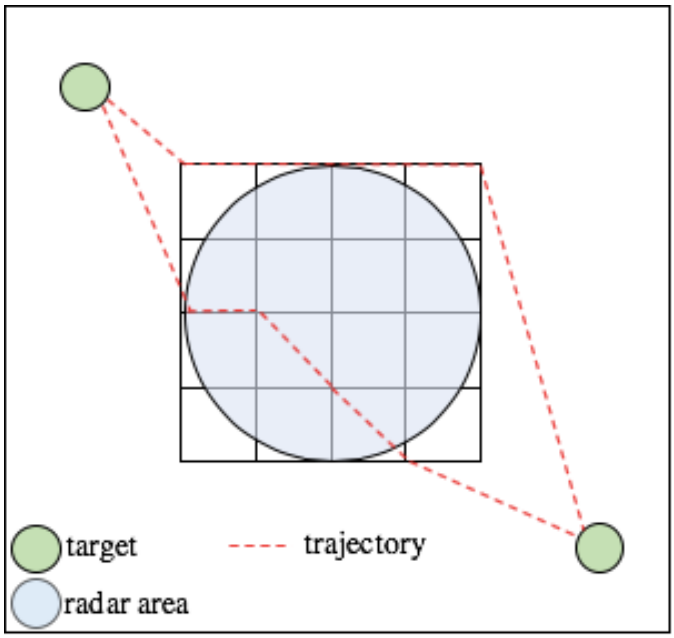

Figure 3.2. Trajectory representation

Let K be the efficient trajectory set, in in the sense of the Definition 3.2, between targets i and j. In that case, the total distance traveled by the fleet is as in Equation (3.4).

$$d = \sum_{i \in I} \sum_{j \in I} \sum_{k \in K} \sum_{u \in U} d_{ijk} X_{ijku} \tag{3.4}$$

where,

d_{ijk}: distance of trajectory $k \in K$ between targets $i \in I$ and $j \in I$

$$X_{ijku} = \begin{cases} 1 & if\ UAV\ u\ flies\ from\ target\ i\ to\ target\ j\ using\ trajectory\ k \\ 0 & otherwise \end{cases}$$

3.2.2. Reward

As mentioned in Section 3.2.1, there is a flight distance limit on UAVs according to their flight duration capability. Hence, it may not be possible for the fleet to visit all predefined targets that have different importance values. Consequently, UAVs aim to maximize the total reward collected within the flight limit as one of the objectives of the problem. Total

reward collected from the targets by the fleet of UAVs is the sum of assigned significance values of targets in each route of every UAV in the fleet.

Since appearance of radar in the terrain does not affect the total reward collected from targets, Equation (3.5) is the same in both versions of the problem.

$$p = \sum_{i \in I} \sum_{j \in I} \sum_{u \in U} p_i \, X_{iju} \tag{3.5}$$

where,

p_i : reward for target $i \in I$

3.2.3. Radar

In military operations, if UAVs are detected by the enemy, risk of being shot increases while traveling in monitored areas and this can lead to failure of the mission and loss of UAVs. UAVs avoid flying through the threats to reduce the exposure level and moves away from them. Thus, UAVs are forced to follow a longer route. The longer route also increases the time UAVs spend on the mission. The third objective of this study is minimizing the total radar detection threat that the fleet is exposed to, without exceeding the flight distance limit on each UAV.

Radar detection threat calculation is adapted from the study of Tezcaner and Köksalan (2011) which considered monostatic radar calculation of Gudaitis (1994). The signal-to-noise (S / N) ratio is used for calculating the probability of detection at each point in the terrain. The S / N ratio is given in Equation (3.6).

$$S/N = \frac{P_t \, G_t^2 \, \lambda^2 \, \sigma}{(4\pi)^3 \, K \, T_s \, B_n \, L_t^2 \, R^4} \tag{3.6}$$

where;

"P_t : power transmitted by radar (watts)

G_t : power gain of transmitting antenna

λ : wavelength of signal frequency (meters)

σ : aircraft radar cross section (RCS) (square meters)

K : Boltzmann's constant (joules/Kelvin)

T_s : receive system noise temperature (Kelvin)

B_n: noise bandwidth of receiver (Hertz)

L_t: transmitting system loss

R : distance from the radar to aircraft"

Constants of Equation (3.6) are combined under the heading C as shown in Equations (3.7) and (3.8).

$$C = \frac{P_t\, G_t^2\, \lambda^2\, \sigma}{(4\pi)^3\, K\, T_s\, B_n\, L_t^2} \tag{3.7}$$

$$S / N = \frac{C}{R^4} \tag{3.8}$$

As can be deduced from Equation (3.8), *S / N* ratio is inversely proportional to R, which means as the distance between radar and the UAV gets longer, value of S/N decreases.

The *S / N* ratio is used to measure the detection probability, p_d. The calculation of the detection probability is also adjusted from the study of Tezcaner and Köksalan (2011) which is given in Equation (3.9).

$$p_d = \begin{cases} 1 & if\ S/N > 30 \\ (S/N - 15)/_{15} & if\ 15 < S/N \leq 30 \\ 0 & if\ S/N \leq 15 \end{cases} \quad (3.9)$$

As S / N ratio increases, meanly the UAV gets closer to the radar, radar detection probability, p_d, converges to 1. In contrast, as the UAV gets away from the radar, radar detection probability converges to 0. After a certain distance, radar cannot detect the UAV.

Due to formulas (3.8) and (3.9), the radars have a circular effective area. To simplify the computations for finding the efficient trajectories, we divide the radar region into grids as shown in Figure 3.3. The detection probabilities of all grid points are calculated using Equation (3.9).

In order to calculate the radar detection threat level UAVs are exposed to during the flight between two grid points i and j (represented in Figure 3.3), arithmetic average of the detection probabilities of these two points are calculated, then this average value is multiplied with the Euclidean distance between points i and j. This calculation is given in Equation (3.10). As stated in Assumption 3.1 and described in Section 3.2.1., since UAVs move with constant speed, the distance traveled can represent the flight duration. Thus, d_{ij} can be used as an estimate of the travel time between points i and j. The measure given in Equation (3.10) estimates the duration the UAV is exposed to the average detection probability of points i and j.

$$r_{ij} = \frac{\left[(p_d)_i + (p_d)_j\right]}{2} \times d_{ij} \quad (3.10)$$

where,

r_{ij} : radar detection threat level exposed by UAV during the flight between two grid points i and j

$(p_d)_i$: radar detection probability at grid point i

$(p_d)_j$: radar detection probability at grid point j

d_{ij} : Euclidean distance between grid points i and j

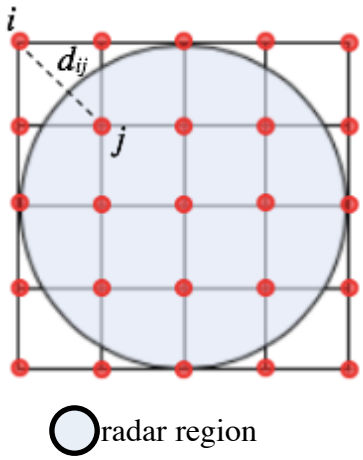

Figure 3.3. Grid representation of radar region

In order to find the radar detection threat of a trajectory between target i and j, radar detection threat levels of grid points used in a trajectory are summed. Consequently, the objective function showing the total radar detection threat is as in Equation (3.11).

$$r = \sum_{i \in I} \sum_{j \in I} \sum_{k \in K} \sum_{u \in U} r_{ijk} X_{ijku} \tag{3.11}$$

where,

r_{ijk} : radar detection threat level of a trajectory k between targets i and j

$$X_{ijku} = \begin{cases} 1 & if\ UAV\ u\ flies\ from\ target\ i\ to\ target\ j\ using\ trajectory\ k \\ 0 & otherwise \end{cases}$$

3.3. Movement of UAVs

In this thesis, for the simplicity, it is assumed that the UAVs move in a two-dimensional area. The problem is decomposed into two as two-criteria and three-criteria versions. In the two-criteria version of the problem, there are no radars monitoring the terrain. In the three-criteria version, terrain includes radars. UAVs make two types of moves with respect to whether there exist radars or not.

3.3.1. Terrain without Radar

In the terrain without radar, UAVs move in continuous space. Hence, the shortest distance is only one efficient trajectory between pairs of targets. A simple representation of movement of UAVs is given in Figure 3.4.

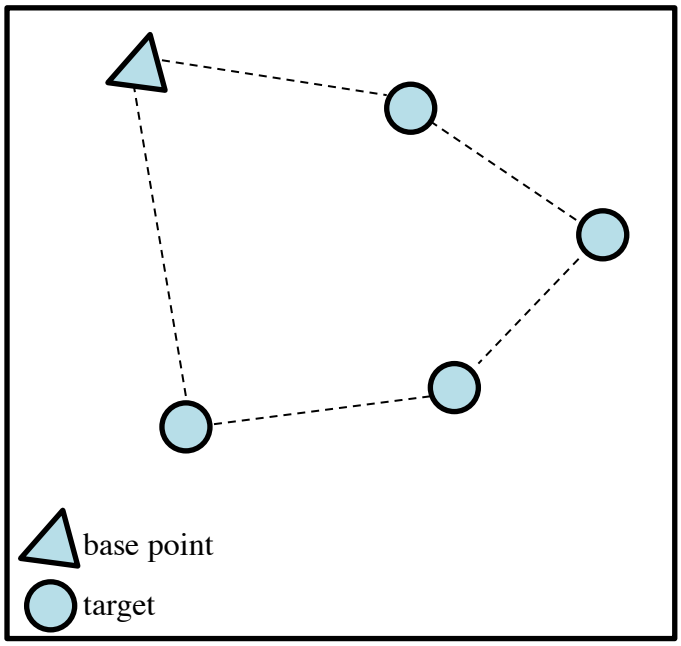

Figure 3.4. Movement of UAV in the terrain without radar

3.3.2. Terrain with Radar

In the terrain with radar, UAVs move in continuous space in the regions where the radars are ineffective. In the effective areas, UAVs follow paths that both minimize the distance traveled and the radar detection threat. In this thesis, radar area is divided by grids as explained in Sections 3.2.1 and 3.2.3. When UAVs enter the radar area they can only

make 45 and 90 degree turns from a horizontal movement and it is possible for UAVs to move to all adjacent grid points. A simple representation of movement of an UAV in a radar region is given in Figure 3.5, green points in the figure show the possible grid points the UAV can fly to.

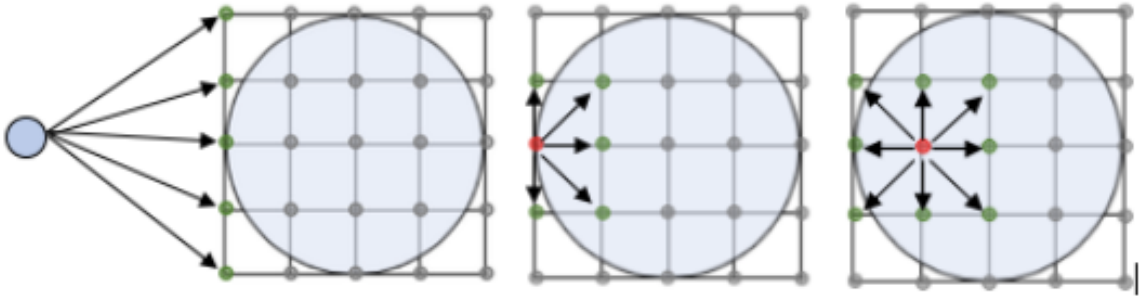

Figure 3.5. Movement of UAV in the terrain with radar

4. METHODOLOGY

In two-criteria version of the problem, we aim to identify the targets of each UAV will visit and visiting order of these targets and in three-criteria version we additively aim to define the paths used between any pair of targets. In order to accomplish these aims, we employ two solution approaches. One is finding exact solutions with mathematical model. However, as problem size (number of UAVs in the fleet, number of targets in mission area) gets larger, finding exact solutions through mathematical models takes much more time than acceptable, since routing missions are usually required to be done in the shortest time. Hence, the other approach is determined as an evolutionary approach, adjusted NSGA-II, to find quick efficient solutions.

4.1. Mathematical Models

In his study, Yakıcı (2016) defines routing part of his problem as Team Orienteering Problem, since maximizing of the total score collected from points of interest visited by UAVs is aimed. Team Orienteering Problem, which is actually an outdoor sport that expects a team including several competitors to collect as many awards from control points within the prescribed time limit, is explained in detail in the study of Chao et al. (1996). In this thesis, we also take the routing problem of a fleet of UAVs into consideration as a Multi-Objective Team Orienteering Problem (MOTOP). We next explain the Mixed Integer Linear Programming (MILP) models developed for the two and three-criteria versions of the problem.

4.1.1 Mathematical Model of the Two-Criteria Version of the Problem

The mathematical model that finds the route for each UAV in the fleet for the two-criteria version of the problem is as follows:

Sets:

U : set of UAVs

I : set of targets and base {0}

Parameters:

d_{ij} : Euclidean distance between targets $i \in I$ and $j \in I$

p_i : reward for target $i \in I$

d_{max} : maximum distance for each UAV

Variables:

X_{iju} : 1 if UAV $u \in U$ flies from target $i \in I$ to target $j \in I$, 0 otherwise

Model:

$$\max \sum_{i \in I} \sum_{j \in I} \sum_{u \in U} p_i X_{iju} \tag{4.1}$$

$$\min \sum_{i \in I} \sum_{j \in I} \sum_{u \in U} d_{ij} X_{iju} \tag{4.2}$$

subject to:

$$\sum_{j \in I \setminus \{0\}} X_{0ju} \leq 1 \qquad \forall u \in U \tag{4.3}$$

$$\sum_{i \in I} \sum_{j \in I} X_{iju} \, d_{ij} \leq d_{max} \qquad \forall u \in U \tag{4.4}$$

$$\sum_{i \in I,\ i \neq j} X_{iju} = \sum_{i \in I,\ i \neq j} X_{jiu} \qquad \forall j \in I, u \in U \tag{4.5}$$

$$\sum_{i \in I} \sum_{u \in U} X_{iju} \leq 1 \qquad \forall j \in I \setminus \{0\} \tag{4.6}$$

$$u_i - u_j + \sum_{i \in I} \sum_{j \in I} (|I| - 1) X_{iju} \leq |I| - 2 \qquad \forall j \in I \setminus \{0\}, i \neq j, u \, U \tag{4.7}$$

$$1 \leq u_i - u_j \leq |I| - 1 \tag{4.8}$$

There are two objective functions in the model, the first one is (4.1), maximizing the sum of visited targets' rewards and the second one is (4.2), minimizing the sum of Euclidean distances between visited targets and the base. Constraint (4.3) indicates that every UAV can leave the base at most once, and constraint (4.4) ensures that each UAV can travel up to a distance. Constraint (4.5) makes sure that a UAV turns back to the base if it leaves the base, if a UAV flies to a target, it has to leave that target, and eliminates the self-loops. Constraint (4.6) guarantees a target can only be visited once by at most one UAV and constraints (4.7) and (4.8) eliminate the subtours.

The mathematical model gives the route for each UAV in the fleet, determines which UAV will visit which of the targets and the order.

4.1.2 Mathematical Model of the Three-Criteria Version of the Problem

In the three-criteria version of the problem, there can be more than one efficient trajectory between pair of targets due to existence of radars in the mission area. Therefore, efficient trajectories between targets need to be found firstly. Finding the efficient trajectories between pair of targets can be considered as a Multi-Objective Shortest Path Problem (MOSPP). We then use a subset of these efficient trajectories in forming the routes.

Before determining the efficient trajectories between targets, they need to be classified. Between a pair of targets, if the shortest-length trajectory intersects with the radar region, there are six possible cases for the type of intersection:

1. There is just one single radar region between the pair of targets and the targets are outside the radar region. A basic representation is given in Figure 4.1.

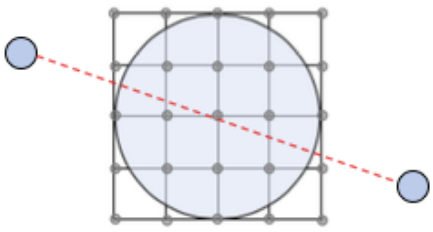

Figure 4.1. Type1 intersection

2. There is just one single radar region between the pair of targets and one of the targets is inside the radar region. A basic representation is given in Figure 4.2.

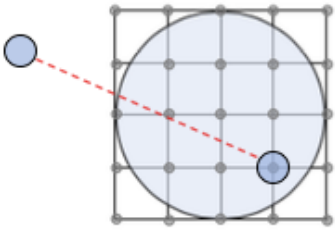

Figure 4.2. Type2 intersection

3. There is just one single radar region between the pair of targets and both of the targets are inside the effect area. Figure 4.3 shows a basic representation.

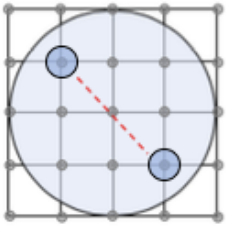

Figure 4.3. Type3 intersection

4. There are multiple radar regions between the pair of targets and the targets are outside the effect area, a basic representation of which is given in Figure 4.4.

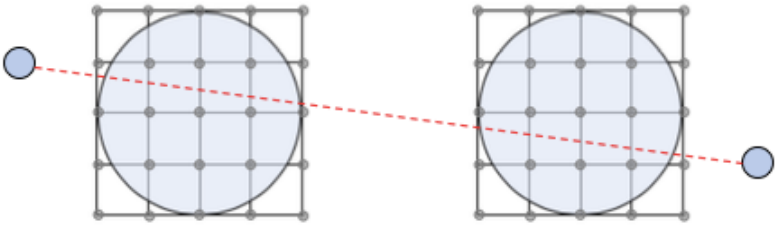

Figure 4.4. Type4 intersection

5. There are multiple regions between the pair of targets and one of the targets is inside the effect area, a basic representation of which is given in Figure 4.5.

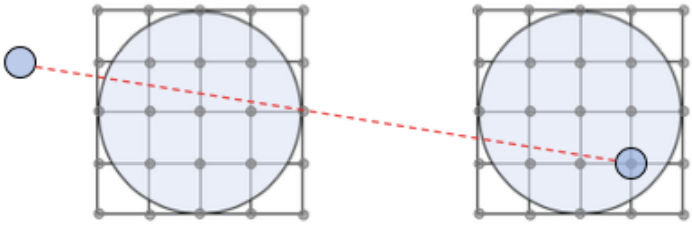

Figure 4.5. Type5 intersection

6. There are multiple radar regions between pair of targets and each target is inside one of the radar regions, a basic representation of which is given in Figure 4.6.

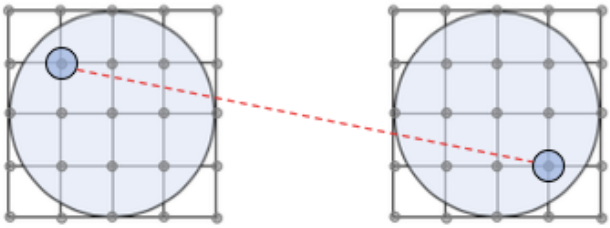

Figure 4.6. Type6 intersection

4.1.2.1. Multi-Objective Shortest Path Problem

According to the intersection types, an adjusted Multi-Objective Shortest Path model is generated for each, which tries to find efficient trajectories between pairs of targets considering minimizing total distance and radar detection threat together and movement constraints of UAV which are explained in Chapter 3. Each radar region is divided into *mxm* gridlines that result in *mxm* grid points that are the intersection points of the gridlines. We also include the two targets as two additional grid points. For *r* radars between any two targets, we have *rxmxm*+2 grid points. We refer to the grid points as nodes in the mathematical model, that is given in detail below.

Sets:

N : node set

s : starting node (first target)

t : terminal node (second target)

d_{ij}: distance from node i to node j

r_{ij} : radar threat value of the shortest-length path between nodes i and j

Variables:

X_{ij} : 1 if path is used between node i and j, 0 otherwise

Model:

$$\min \sum_{i \in N} \sum_{j \in N} d_{ij} X_{ij} \tag{4.9}$$

$$\min \sum_{i \in N} \sum_{j \in N} r_{ij} X_{ij} \tag{4.10}$$

subject to:

$$\sum_{j \in N \setminus \{s\}} X_{sj} = 1 \tag{4.11}$$

$$\sum_{j \in N \setminus \{t\}} X_{jt} = 1 \tag{4.12}$$

$$\sum_{i \in N \setminus \{t\}} X_{ij} - \sum_{i \in N \setminus \{s\}} X_{ij} = 0 \qquad \forall j \in N \setminus \{s, t\} \tag{4.13}$$

$$X_{ij} \in \{0, 1\} \tag{4.14}$$

There are two objectives considered in the model which are shown by equations (4.19) and (4.10), minimizing total distance and total radar detection threat of trajectory between targets s and t, respectively. Constraints (4.11), (4.12) and (4.13) guarantee that one unit flows from s to t. Constraint (4.14) ensures that if trajectory includes the path between nodes i and j, the variable X_{ij} gets the value of 1; otherwise it gets the value of 0.

We find k efficient trajectories between a pair of targets, each having a better distance or radar detection threat value if there is a radar region between them. These efficient trajectories are used as input while finding route of each UAV.

4.1.2.2. Finding the Routes of a Fleet of UAVs

In order to solve the three-objective version of the problem, we use an extended version of the mathematical model given in Section 4.1.1. Index k is added which represents the k^{th} efficient trajectory between targets. Distance parameter and decision variable is updated with newly added index, and third objective is adjoined as minimizing total radar threat value. The mathematical model in detail is as follows

Indices and sets:

$k \in K_{ij}$: set of efficient trajectories between targets $i \in I$ and $j \in I$

Parameters:

d_{ijk} : distance of trajectory $k \in K_{ij}$ between targets $i \in I$ and $j \in I$

r_{ijk} : radar threat value of trajectory $k \in K_{ij}$ between targets $i \in I$ and $j \in I$

Variables:

X_{ijku} : 1 if UAV $u \in U$ flies from target $i \in I$ to target $j \in I$ using trajectory $k \in K_{ij}$, 0 otherwise

Model:

$$\max \sum_{i \in I} \sum_{j \in I} \sum_{u \in U} \sum_{k \in K_{ij}} p_i X_{ijku} \tag{4.15}$$

$$\min \sum_{i \in I} \sum_{j \in I} \sum_{u \in U} \sum_{k \in K_{ij}} d_{ijk} X_{ijku} \tag{4.16}$$

$$\min \sum_{i \in I} \sum_{j \in I} \sum_{u \in U} \sum_{k \in K_{ij}} r_{ijk} X_{ijku} \tag{4.17}$$

subject to:

$$\sum_{j \in I \setminus \{0\}} \sum_{k \in K_{ij}} X_{0jku} \leq 1 \qquad \forall u \in U \quad (4.18)$$

$$\sum_{j \in I} \sum_{i \in I} \sum_{k \in K_{ij}} X_{ijku}\, d_{ijk} \leq d_{max} \qquad \forall u \in U \quad (4.19)$$

$$\sum_{i \in I,\ i \neq j} \sum_{k \in K_{ij}} X_{ijku} = \sum_{i \in I,\ i \neq j} \sum_{k \in K_{ij}} X_{jiku} \qquad \forall j \in I, u \in U \quad (4.20)$$

$$\sum_{i \in I} \sum_{k \in K_{ij}} \sum_{u \in U} X_{ijku} \leq 1 \qquad \forall j \in I \setminus \{0\} \quad (4.21)$$

$$u_i - u_j + \sum_{i \in I} \sum_{j \in I} \sum_{k \in K_{ij}} (|I| - 1) X_{ijku} \leq |I| - 2 \qquad \forall j \in I \setminus \{0\}, i \neq j, u \in U \quad (4.22)$$

$$1 \leq u_i - u_j \leq |I| - 1 \quad (4.23)$$

Equations (4.16), (4.17) and (4.18) represent the three objectives of the problem, maximizing the total reward collected from targets visited, minimizing total distance traveled by the fleet and minimizing total radar detection threat, respectively. Other constraints serve for the same purposes as in Section 4.1.1.

The three-objective mathematical model finds the route for each UAV in the fleet, determined which UAV will visit which of the targets, in what order and using which trajectory between targets.

4.2. Evolutionary Approach

Our mathematical model can find efficient solutions for small sized problems in a reasonable time. However as problem gets larger, run time of the mathematical model cascades. In this thesis, to approximate the efficient solutions of the problem quickly, an evolutionary approach, NSGA-II is applied to the problem.

Evolutionary Algorithms (EAs) have been stimulated from the biological evolution process and mechanisms. EAs are based on the "survival of the fittest" phenomena of Darwin's evolutionary theory. The algorithm basically starts with generating an initial population and continues generating offspring from this population using a crossover operator. Afterwards, some offspring are mutated and all population is evaluated. In the evaluation process, the fittest members of the population continue to stay in the population while the worst ones are eliminated. The population converges to fitter members as the generations progress.

In his book, Deb (2001) claims that an exclusive characteristic of the evolutionary optimization is finding and maintaining multiple solutions in a single simulation run. Therefore, EAs are widely used in multi-objective optimization problems. He also indicates that in multi-objective optimization , there are two purposes which are finding a solution set as diverse and close to the Pareto-optimal front as possible. Deb (2001) classifies Multi-Objective Evolutionary Algorithms (MOEAs) as elitist and non-elitist. Elitist MOEAs differ from non-elitist MOEAs by an elite-preserving operator favoring the elites (best non-dominated solutions) of the population by giving them the opportunity to be transferred directly to the next generation. Among elitist MOEAs, NSGA-II is applied to our problem.

4.2.1 Elitist Non-Dominated Sorting Genetic Algorithm (NSGA-II)

NSGA-II is an elitist MOEA proposed by Deb et al. in 2000, that also uses an "explicit diversity-preserving mechanism". NSGA-II creates the offspring population of N individuals, Q_t, from the parent population of N individuals, P_t, by using evolutionary operators (crossover, mutation). These two populations together constitute the entire population of $2N$ individuals, R_t. Then, R_t is classified using non-dominated sorting, which sorts solutions into fronts according to domination, the solutions in better fronts dominate the solutions in other fronts. The new population, having N individuals (slots), is filled with solutions of non-dominated fronts, one at a time starting with the first (best) front. While filling the new population, if the number of remaining slots are less than the solutions in the queued front, crowding distance sorting is applied to that front for sorting through the solutions. Crowding distance is a diversity measure that shows the distance

between a solution and its closest solutions. A higher crowding distance indicates that the solution does not have too many close solutions, so that the higher the crowding distance is, the better the solution is. An overview of this procedure can be seen in Figure 4.7 (Deb, 2001).

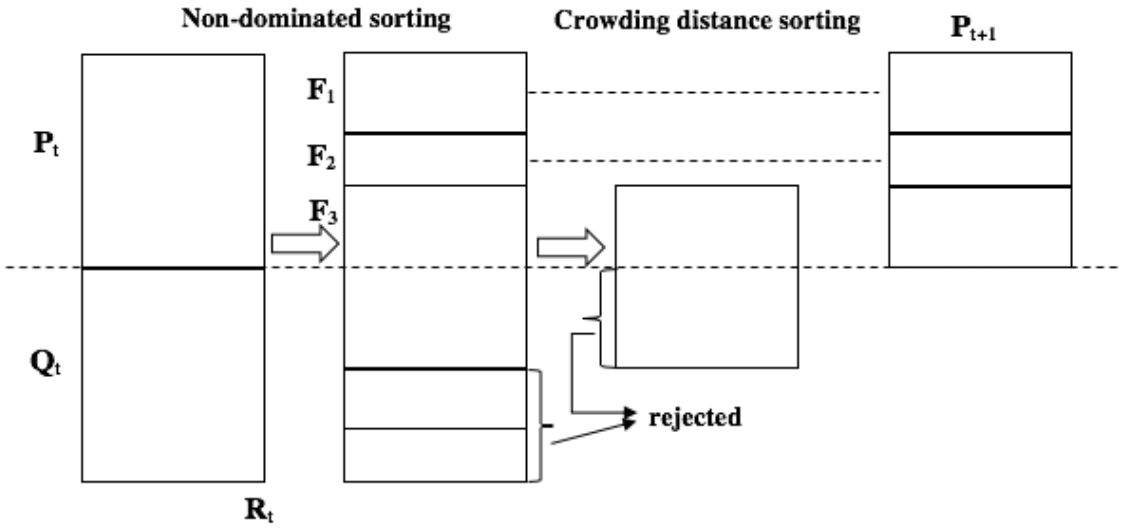

Figure 4.7. Schematic representation of the NSGA-II procedure

We develop mechanisms for NSGA-II that address the two and three-objective versions of our problem, separately. Basically, there are differences in the chromosome representation and the evolutionary operators between the two problems. In Figure 4.8, an overall review of the NSGA-II procedure, which is adjusted from the study of Deb et al. (2002), is given. Detailed explanation of the differences and functions in NSGA-II are explained next.

Procedure NSGA-II

1: Initialize random population - size *N*

2: Evaluate objective values of initial population

3: Assign rankings depend on Pareto dominance - sort

4: Generate population of offspring

5: Tournament Selection

6: Crossover and Mutation

7: **for** *i* = 1 *to generation number* **do**

8: **for** every parent and offspring in population **do**

9: Assign rankings depend on Pareto dominance - sort

10: Generate sets of nondominated solutions

11: Determine crowding distance

12: Loop (inside) by adding solutions from the first front to *N* individuals in the next generation

13: **end for**

14: Choose points (elitist) at the lower front (with lower rank) with high crowding distance

15: Constitute next generation

16: Tournament Selection

17: Crossover and Mutation

18: **end for**

Figure 4.8. NSGA-II Procedure

4.2.1.1 NSGA-II for the Two-Criteria Version of the Problem

In comparison with traditional NSGA-II, some modifications are made to customize it for the multi-objective fleet routing problem. We refer to our algorithm as EA-fUAV (Evolutionary Approach for routing a fleet of UAVs). A specialized chromosome representation is developed for the problem. Crossover and mutation operators are adjusted according to the chromosome structure. A specialized initialization procedure is developed to generate better initial population. Furthermore, since there is a distance limitation on each UAV, during initialization and after crossover and mutation operations, route of each UAV is arranged with Nearest Neighbor (NN) Algorithm to lower the distance. After application of the NN, if there are still routes that exceed the maximum distance limit, a repair procedure is applied to them. All these modifications are explained in the upcoming sections in detail.

Chromosome representation

Each solution of the routing problem is referred as a chromosome. Chromosome structure is designed to include a route for each UAV in the fleet. In Figure 4.9, an example chromosome representation is given for a fleet of three UAVs. The routes of the UAVs is separated by zeros in the chromosome, this means UAV1 leaves from the base, visits target 10 and turns back to the base. At the same time, UAV2 leaves from the base, visits targets 13, 2, 7 and 3 in this order and returns to the base. UAV3 leaves from the base, visits targets 5, 4 and 12 and turns back to the base. Chromosome representation is updated according to the number of targets and UAVs in the fleet.

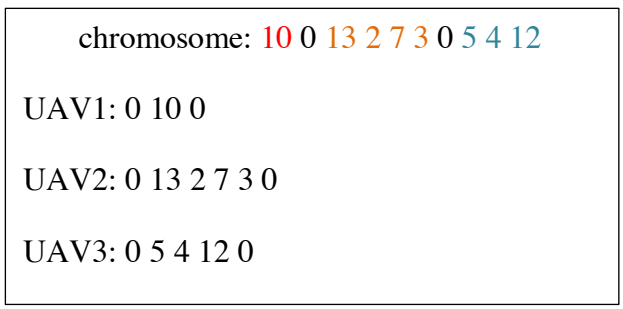

Figure 4.9. Chromosome representation

Initialization

At the stage of initialization, it is needed to generate an initial population size of *N*. Initial population includes randomly-generated members. The procedure of initialization used in this thesis is explained in Figure 4.10.

Procedure Initialization

Generate *N* chromosomes (solutions) including genes of size [number of targets + (number of UAVs in the fleet – 1)]

1: **for** *i*=1 to *N*
2: Randomly order numbers from 1 to target number, *C*
3: Assign (number of UAVs in the fleet – 1) zeros randomly in the ordered numbers in array *C*
4: Organize each UAV's route using *NN Algorithm (explained below)*
5: **if** total distance of UAV route > maximum distance limit **do**
6: **repeat**
7: Eliminate one of the targets in the route randomly
8: Re-organize the route with *NN Algorithm*
9: **until** total distance of UAV ≤ maximum distance limit
10: **end if**
11: **end for**

Figure 4.10. Initialization procedure

Nearest Neighborhood Algorithm

Once a UAV is assigned a set of targets, we find the visiting order of the targets using the Nearest Neighborhood Algorithm (NN Algorithm), (Winston, 2004), in the process of initialization and after the mutation and crossover operators . The algorithm starts with choosing a random target from the route of the UAV, that chosen target is visited first after taking off from the base. Remaining targets in the route of the UAV are ordered according to being nearest to the predecessor target until all targets in the route are ordered.

Crossover

Traditional crossover operator is adjusted for the routing problem. For any two solutions, firstly, a UAV's route is chosen randomly . Then, a random place is selected for each of these routes and the two routes are swapped from these places. An example is shown in Figure 4.11. Second UAV's routes are chosen from Solutions 1 and 2, and these routes are swapped from the underlined places. Then, crossover applied routes are added to their places. If, as a result, one offspring visits a target twice, the target is removed from the first UAV that visits it.

Solution 1: 2 0 9 0 7

Solution 2: 4 0 12 13 3 0 15 5 1

Route 1: 9

Route 2: 12 13 3

Offspring 1: 2 0 13 3 0 7

Offspring 2: 4 0 12 9 0 15 5 1

Figure 4.11. Crossover example

Mutation

A specific mutation operator is applied with respect to the chromosome representation. With the mutation operator, we aim to visit more targets for each UAV. The procedure is given in Figure 4.12

Procedure Mutation

```
1:  for  i=1 to N
2:  Determine the unvisited targets in chromosome i
3:  Decompose chromosome into UAV routes
4:      for each UAV route
5:          if generated probability ≤ mutation probability do
6:              Choose one of the unvisited targets randomly
7:              Assign that target in a random place in the route
8:          end if
9:      end for
10: end for
```

Figure 4.12. Mutation procedure

Repair Procedure

After crossover, mutation operators and NN algorithm, the distance traveled by each UAV in every chromosome/solution is calculated. If in any of the solutions there is a UAV that exceeds the maximum distance limit, we follow the procedure given in Figure 4.13.

Procedure Repair Procedure

```
for i=1 to N
Calculate distance traveled by each UAV in chromosome i
  if distance traveled by a UAV > maximum distance limit do
    repeat
      Eliminate one of the targets in the route randomly
      Re-organize the route with NN
    until total distance of UAV ≤ maximum distance limit
  end if
end for
```

Figure 4.13. Repair procedure

4.2.2.1 NSGA-II for the Three-Criteria Version of the Problem

In the three-criteria version of the problem, there are multiple efficient trajectories between pair of targets that should be considered. Therefore, we update some of the functions and operators to include also the trajectory to be used between pair of targets.

Chromosome representation

In this version, the representation of the chromosomes should include the trajectories between targets. For that reason, a second array is added to the representation as shown in Figure 4.14. The first array of the chromosome represents the targets to be visited, and the second row represents the trajectory used between targets. In the example in Figure 4.14, UAV1 takes off from the base, visits target 4 using the first efficient trajectory between the base and target 4, then returns to the base by using the first efficient trajectory again. UAV2 takes off from the base, visits targets 12, 13, 3 and turns back to the base using trajectories 1, 7, 2 and 5, respectively. UAV3 leaves the base to visit targets 15, 5 and 1 using trajectories 1, 1, 3 and 1, respectively.

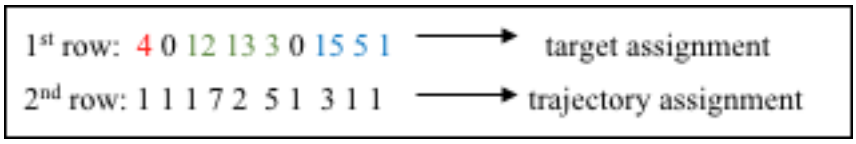

Figure 4.14. Chromosome representation of three criteria

Initialization

Initialization procedure is similar to the two-criteria version for the target assignment. The difference is assigning trajectories for each solution. After assigning the targets to the UAVs, 5 different trajectory options are created for each assignment, increasing the number of solutions from *N* to *5N*. Each of 5 trajectories has a better distance or radar value, in order to generate better solutions. Then, with tournament selection, chromosome number is decreased to *N*.

Crossover

Since chromosome representation is changed, crossover operator is modified for that. Solutions are crossed-over as in the two-objective case, but the newly-formed trajectory pairs are assigned new trajectories randomly.

Mutation

Mutation operator is implemented to the solutions as in the two-objective version, but when a new target is added to the solution, that target is connected with its predecessor and successor targets with trajectories assigned randomly.

Repair Procedure

After initialization and mutation processes, route objective values are checked. If in any of the solutions there is a UAV that exceeds the maximum distance limit, one of the targets in that route is eliminated randomly with the paths related to it. This repair procedure is repeated until distance limitation is satisfied in all routes. In this version, NN algorithm is not employed to re-arrange.

We generate three different problem instances with different numbers of UAVs, targets, and radars. We solve these instances exactly, and using two and three-criteria versions of adjusted NSGA-II. We give the computational results for the instances in the next chapter.

With our solution approaches, different UAV types and radars can also be easily handled. If the UAVs have different speeds and flight limits, we can customize the related parameters and constraints in our approaches for each UAV. Different radar regions can be included in our terrain representation.

5. COMPUTATIONAL STUDY

In order to evaluate the modified NSGA-II on both two and three-objective routing problem of a fleet of UAVs, a 100 km × 100 km mission area is specified, and in this area, three different case studies are generated.

For the radar-free version of the problem, three problem settings with different numbers of targets and UAVs are generated. As we increase the number of UAVs, we also increase the number of targets. In the first case, there are 15 targets randomly located in the mission area; coordinates are produced from uniform distribution within the range [0,100]. 3 UAVs are deployed from the base that is located at the center of the targets. This case is named as "3U15T" regarding its UAV and target number. In the second case, 5 more targets and one more UAV are added to the mission area of the first case. This case includes 4 UAVs and 20 targets, therefore it is named as "4U20T". Lastly in the third case, 5 more targets and one more UAV are considered in addition to the second case. Since there are 25 targets and 5 UAVs in this case, it is named as "5U25T". Distance matrix is constituted including each target pair and base using Euclidean distance. The representation of the first case in the 100 km × 100 km mission area with and without gridlines are given in Figure 5.1 and Figure 5.2, respectively. Every square edge in Figure 5.1 represents one kilometer unit. The representation of the other two cases, 4U20T and 5U25T, are given in Appendices 1 and 2, respectively.

For the three-criteria version of the problem, the same three cases generated for the radar-free version are used exactly with locating 3 radar regions randomly to the mission area. Radar regions are discretized with 16 horizontal and 16 vertical equi-distant gridlines that result in 256 grid points. The discretization is explained in detail in Section 3.3.2. We solve the MOSPP employing the ε-constraint method, (Chankong and Haimes, 1983), to find all efficient trajectories between targets. The shortest path algorithm results are used to fill in the distance matrix. The representation of the first case with radar is given in Figure 5.3 and for other cases Appendices 3 and 4 can be seen.

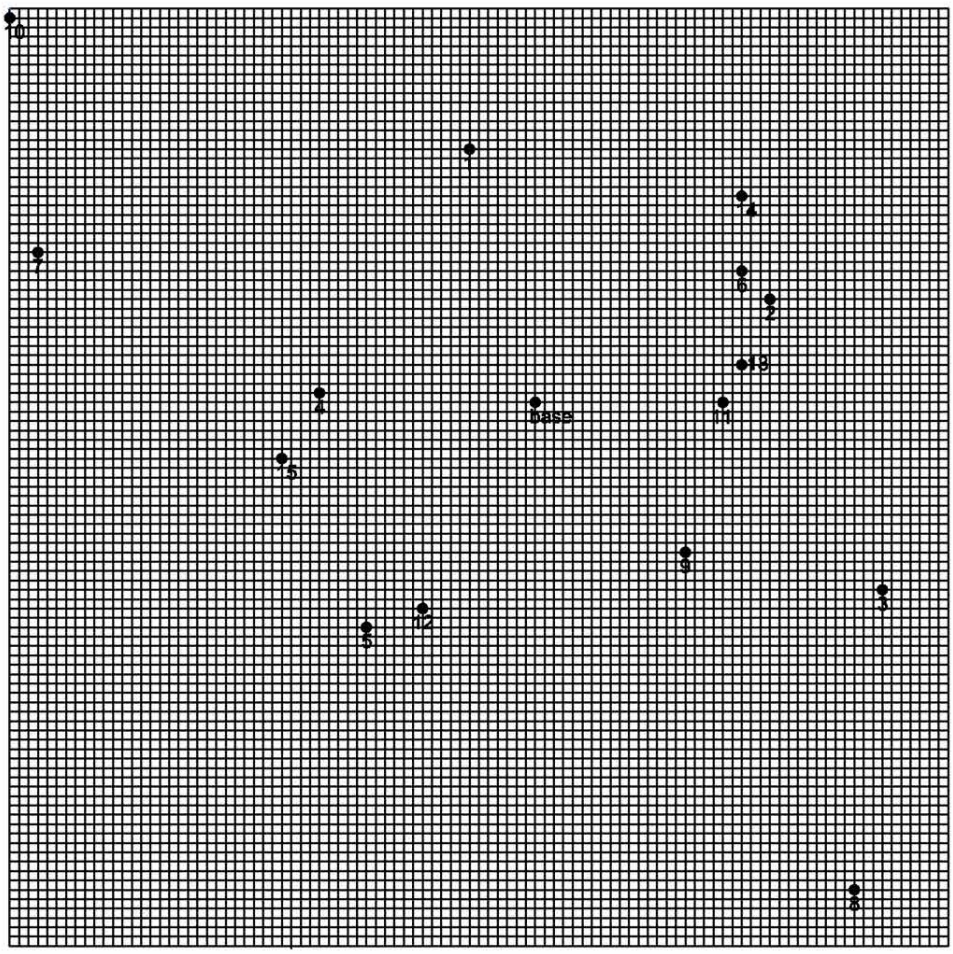

Figure 5.1. Discretized mission area, case 3U15T

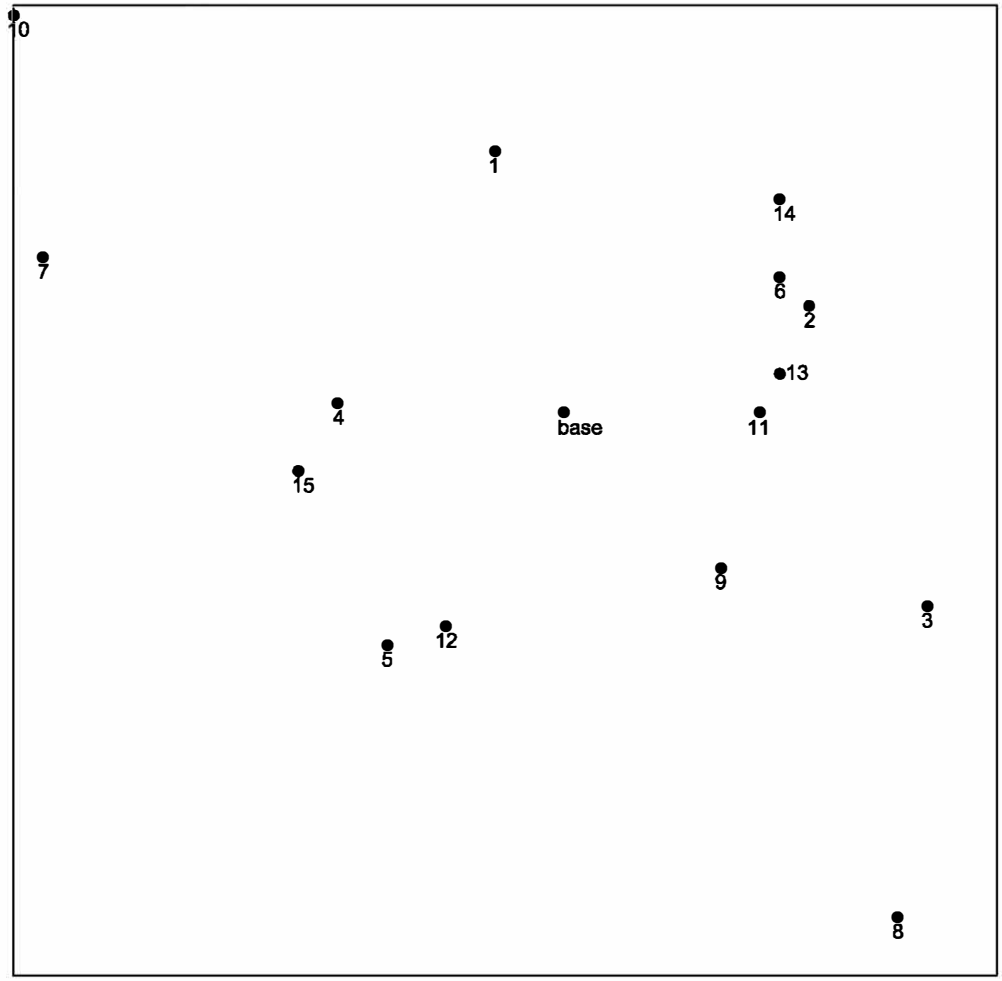

Figure 5.2. Continuous mission area, case 3U15T

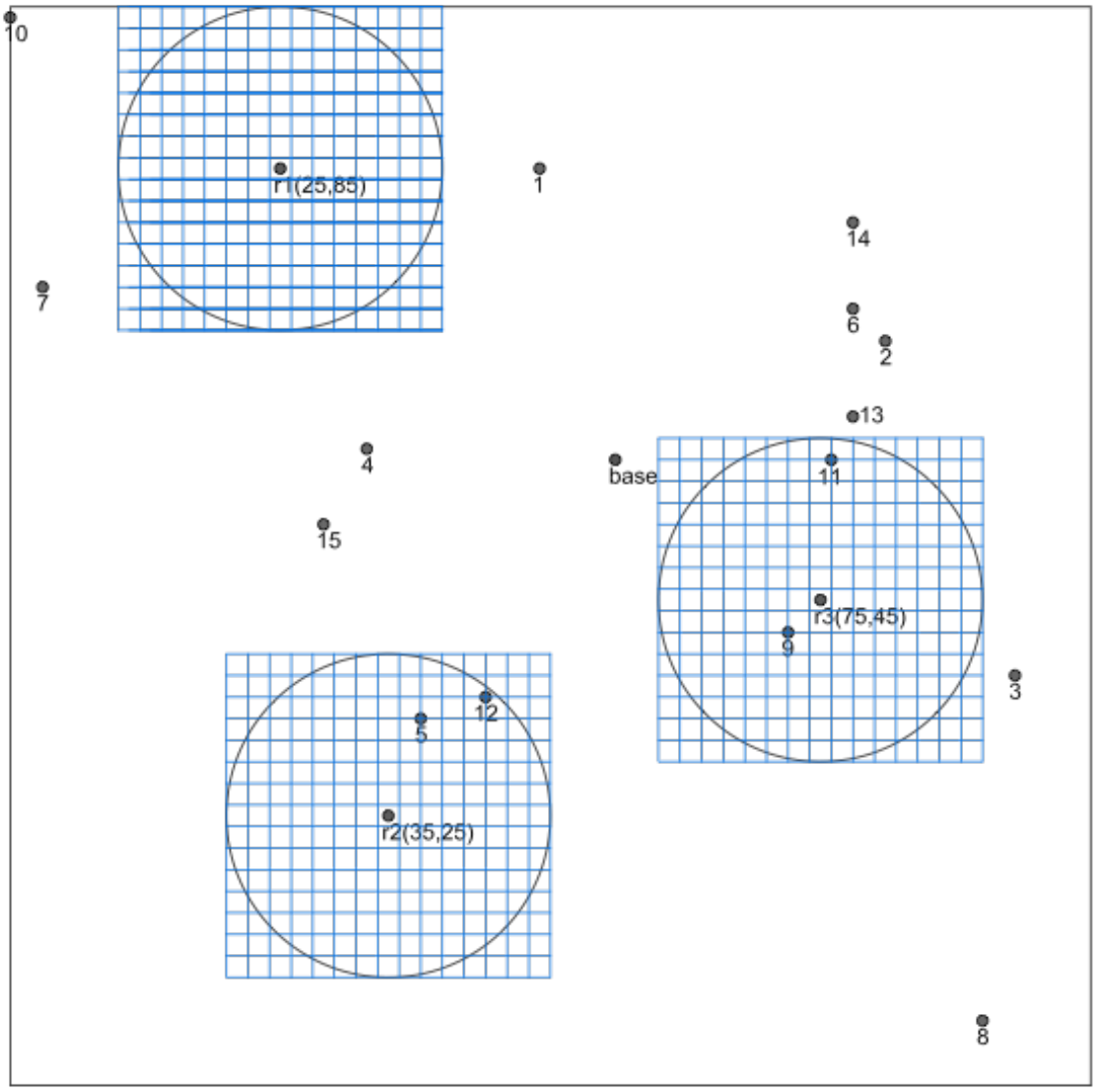

Figure 5.3. Mission area with radar, case 3U15T

Reward values are randomly assigned to each target from uniform distribution with range [1,10]. In each case, every UAV has a 150 km maximum travel distance limit with accepted cruise speed as 60 knot (111.12 km/h) and flight time as 80 minutes.

To find the Pareto optimal front of exact solutions, we solved all cases using ε-constraint method. In the ε-constraint method, one of the objectives is optimized while other objectives are treated as constraints. The limit, ε, on the objectives that are treated as constraints are changed each time to obtain a new solution. Also, other objectives are added to the objective function after being multiplied with a very small coefficient to guarantee obtaining efficient solutions (Mavrotas, 2009). This method is implemented to

the cases in GAMS, using CPLEX solver for mathematical models in Chapter 4. These implementations are performed on a PC with 2.50 GHz Intel Core i5 6500T CPU, 8 GB RAM.

For the suggested modified NSGA-II, we modified the functions of the package 'nsga2R' version 1.0, Elitist NSGA-II based on R, provided at https://cran.r-project.org/web/packages/nsga2R/index.html, which is explained in Chapter 4. These implementations are performed on a PC with 1.6 GHz Intel Core i5 CPU, 8 GB 1600 MHz DDR3 RAM.

Hypervolume Indicator

For the evaluation of suggested modified NSGA-II, EA-fUAV, in order to compare the generated solutions with exact solutions gathered from the mathematical model, hypervolume indicator is used. The hypervolume (HV), which is suggested by Zitzler and Thiele (1999), indicates the volume of the dominated area by the solutions of a front until a reference point. Heuristic solutions, which are found with EA-fUAV, compose the approximate front, and the exact solutions, which are the output of the mathematical model, compose the Pareto optimal front. Van Veldhuizen (1999) proposes the hypervolume ratio (HVR) which is the proportion of HV of the approximate front to the Pareto optimal front. We use HVR to demonstrate the performance of the approximate front found by the suggested heuristic. Bigger HV results in better HVR, and thus better performance of the heuristic. We scaled HVs within the range [0,1] to be more precise and proportion is named as HV indicator. HV indicator values are between 0 and 1. As the approximate solutions gets closer to the exact solutions, HV indicator converges to value 1, which is the ideal case where the approximate and the exact solutions are equal to each other.

5.1 Two-Criteria Version of the Problem

Initially, we generate optimal solutions with ε-constraint method by minimizing the total distance traveled by the fleet in the objective and using the total reward collected by the fleet as a constraint by adjusting the bound on constraint between the extreme points of the total reward. Hence, we get Pareto optimal fronts for the cases.

For the EA-fUAV, we run each case for 500 generations and 5 instances are generated for each case with changing initial parents at each instance. Population size is changed with respect to the number of UAVs and targets in the cases. We take population size as the multiplication of the number of UAVs and targets, e.g. in 3U15T case, population size is 45, whereas it is 80 in 4U20T case. We analyze the performance of the algorithm for all three cases. We compare the approximate front with the Pareto optimal front both visually and with HVR.

3U15T case

In Figure 5.4, the Pareto optimal front of the two-objective case 3U15T is given. Extreme nondominated points are the two solutions with minimum distance (distance is 40 km, reward is 6) and maximum reward (distance is 446.52 km, reward is 86). Note that there is distance limitation on UAVs as 150 km. In the solution with minimum distance, one of the UAVs takes off from the base, visits target 11 and turns back to the base. Representation of the route for the extreme point with maximum reward can be seen in Figure 5.5. Different type of lines represent different UAVs' routes, numbers below and above dots represent the target numbers and the rewards assigned to targets, respectively.

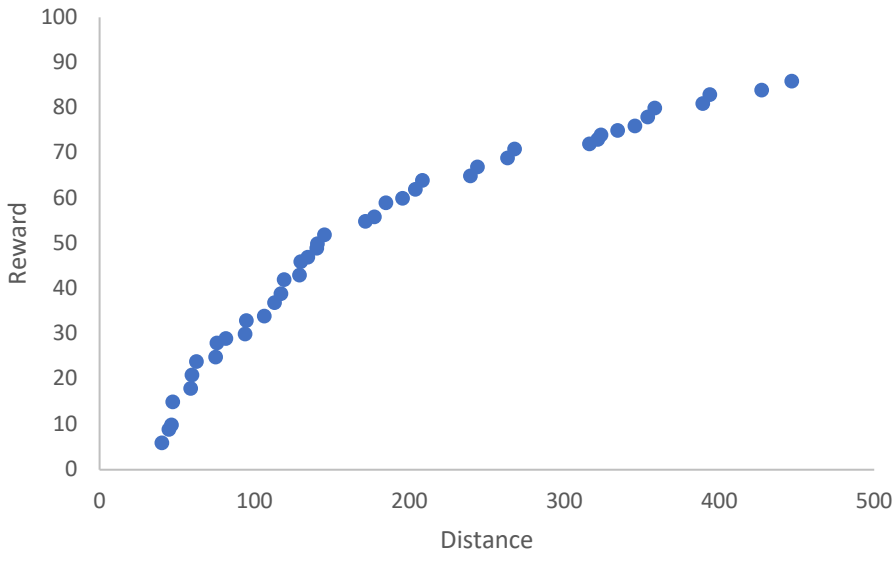

Figure 5.4. Pareto optimal front, case 3U15T

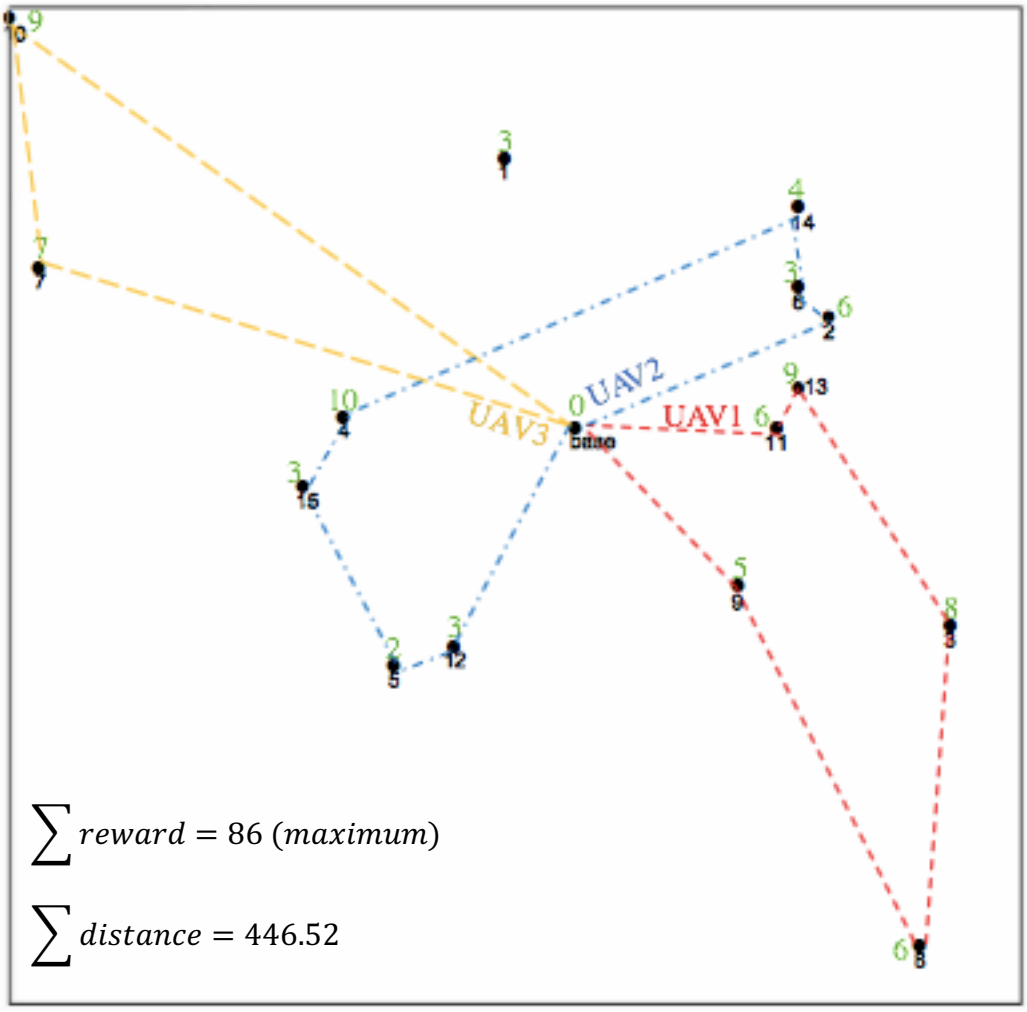

Figure 5.5. Route of the solution with maximum reward, case 3U15T

In EA-fUAV, we firstly set the probability of crossover to 0.7 and probability of mutation (mprob) to 0.2. One of our objectives is maximizing the total reward collected by the fleet, this objective is turned into minimization and both optimal and EA-fUAV results are scaled within [0,1] in order to test HV more precisely. 5 different instances are generated to take an average test result, summary of these instances can be seen in Table 5.1. On average, EA-fUAV results converge to the optimal results with approximately 98.9% rate. However, the extreme point where reward is maximum cannot be covered by the algorithm. Hence, we try two more different mutation probability parameters as 0.4 and 0.6.

Table 5.1. Hypervolume indicator values for the case 3U15T with different mprob parameters

		HV indicator		
case		***mprob=0.2***	***mprob=0.4***	***mprob=0.6***
	minimum	0.9816	0.9725	0.9955
3U15T	**maximum**	0.9973	0.9966	0.9967
	average	**0.9888**	**0.9909**	**0.9961**

Average HV indicator of 5 different instances with mprob=0.4 is calculated as around 99.1%, can be seen on Table 5.1. Further, when mprob is set to 0.6 the average HV indicator of 5 different instances increases into 99.6%. Since there is not a significant difference between average execution times with different probability parameters as seen on

Table 5.2, mprob with the best HV indicator is chosen which is 0.6 and implied in the other cases. Comparison of Pareto optimal front and approximate front with mutation probability 0.6 can be seen in Figure 5.6 and scaled representation can be seen in Figure 5.7.

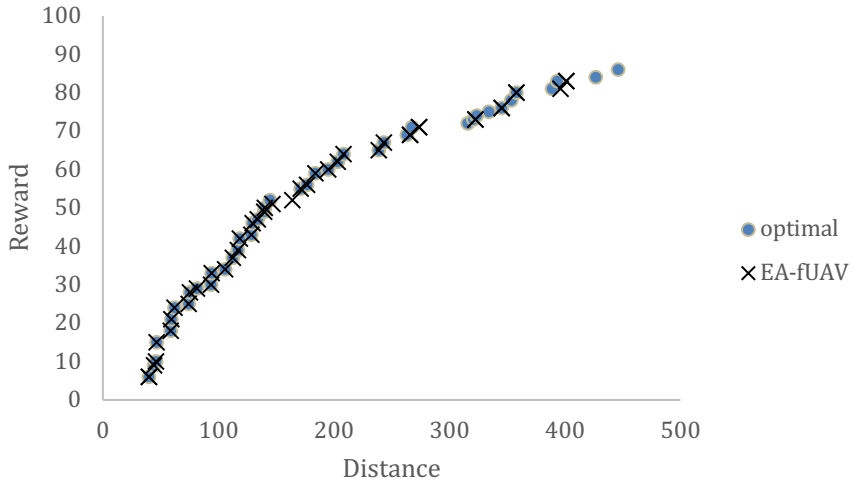

Figure 5.6. Comparison of Pareto optimal front and approximate front with mutation probability 0.6, case 3U15T

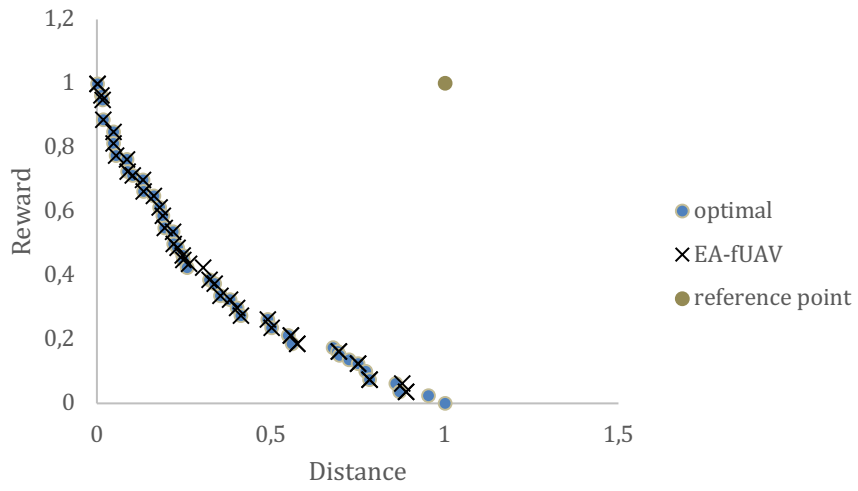

Figure 5.7. Comparison of the scaled Pareto optimal front with the scaled approximate, case 3U15T

Table 5.2. Elapsed execution time values for the case 3U15T with different mprob parameters

		time elapsed-EA-fUAV (sec)		
case		***mprob=0.2***	***mprob=0.4***	***mprob=0.6***
	minimum	20.10	20.60	21.12
3U15T	**maximum**	22.12	22.30	25.14
	average	**20.87**	**21.41**	**22.86**

Since mprob is chosen as 0.6, it would be appropriate to compare execution times of optimal solutions with EA-fUAV results where mprob=0.6. Execution time for finding optimal solutions is approximately 300 times more than the execution time of EA-fUAV, exact values can be seen in Table 5.3.

Table 5.3. Comparison of execution times, case 3U15T

	time elapsed (sec)	
case	***EA-fUAV***	***optimal***
3U15T	22.86	6919.15

4U20T case

In this case, mprob is chosen as 0.6. Figure 5.8 shows the comparison of the Pareto optimal front with the approximate front constituted as a result of an instance of EA-fUAV. In accordance with both graphs in Figure 5.8 and Figure 5.9, it can be said that the right tail of the Pareto optimal front cannot be converged as well as the 3U15T case, HV indicator of the instance confirms this inference with a value of 0.95. Further, as seen in

Table 5.4 5.4, average HV indicator value of 5 instances is 0.94, EA-fUAV results converge to optimal solutions with about 94% coverage.

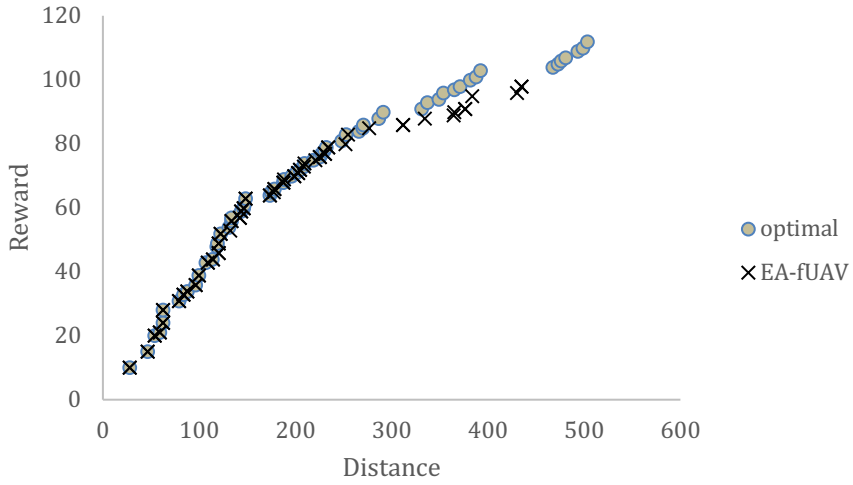

Figure 5.8. Comparison of the Pareto optimal front with the approximate front, case 4U20T

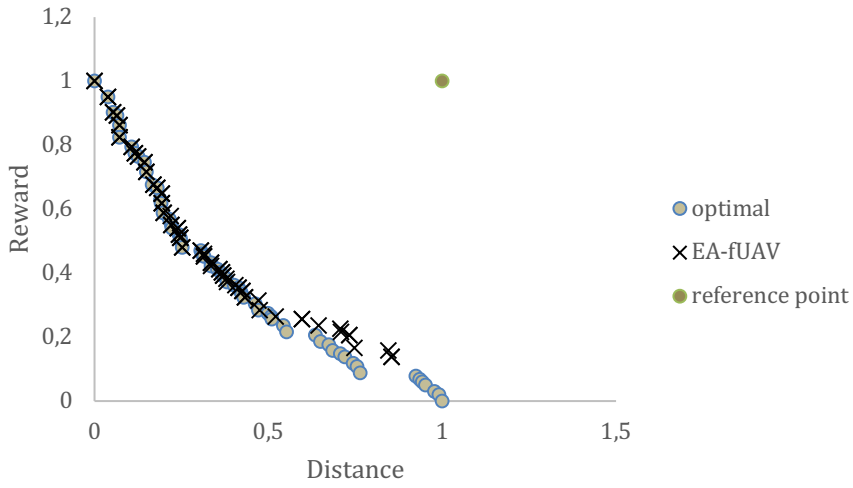

Figure 5.9. Comparison of the scaled Pareto optimal front with the scaled approximate front, case 4U20T

Table 5.4. Hypervolume indicator values for the case 4U20T

case		*HV indicator*	*time elapsed (sec)*
	minimum	0.9048	53.45
4U20T	**maximum**	0.9576	59.84
	average	**0.9414**	**55.43**

There is again a significant difference in execution times as in the 3U15T case, which is given in Table 5.5.

Table 5.5. Comparison of execution times, case 4U20T

	time elapsed (sec)	
case	***EA-fUAV***	***optimal***
4U20T	55.43	22163.34

5U25T case

In this case, mprob is also chosen as 0.6. However, since finding exact optimal solutions in GAMS takes an unacceptable amount of time, the solutions were stopped due to execution time. We gathered results with reward values 103 or lower. Figure 5.10 shows the comparison of the Pareto optimal front with the approximate front constituted of the results of an instance of EA-fUAV. In order to calculate HV indicator in an accurate way, EA-fUAV results are filtered and the ones with reward higher than 103 are eliminated. This procedure is applied to all instances. Scaled graph of the remaining solutions in an instance can be seen in Figure 5.11 .

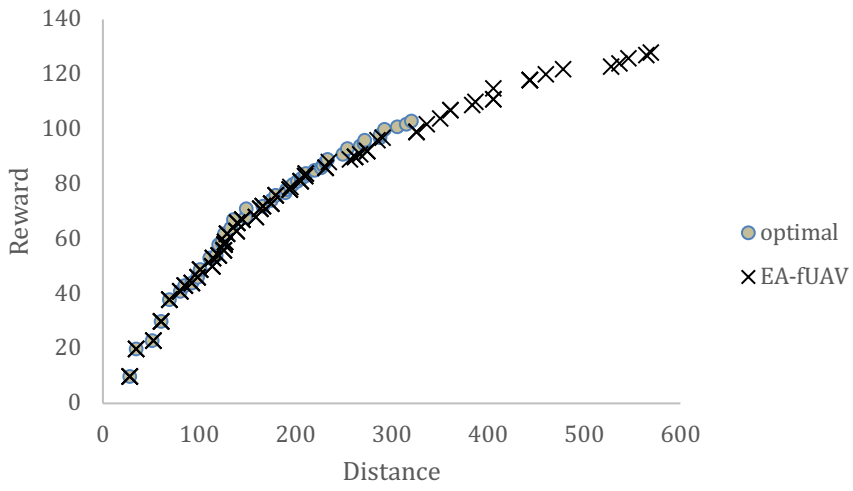

Figure 5.10. Comparison of the Pareto optimal front with the approximate front, case 5U25T

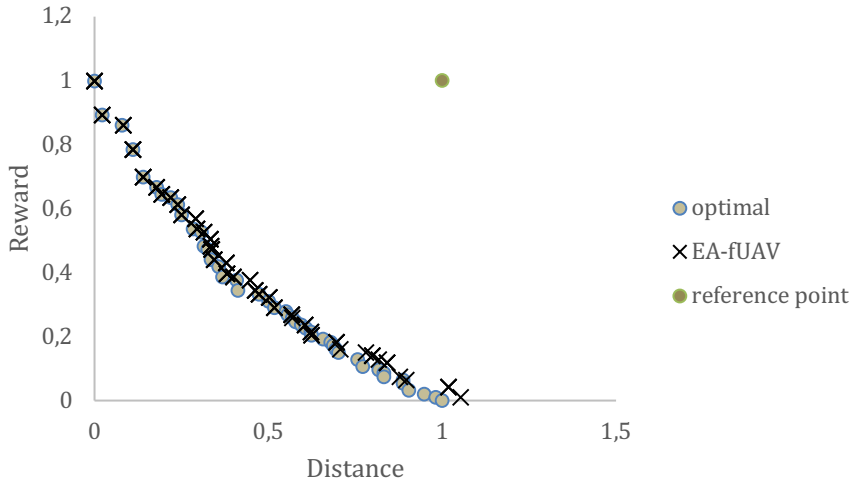

Figure 5.11. Comparison of the scaled Pareto optimal front with the scaled approximate front, case 5U25T

We expected a reduction in HV indicator in comparison to the case 4U20T, however it increased. We thought that the reason could be the increased population size of this case relative to the previous one. However, as seen in Table 5.6, it can be said that population size does not affect HV indicator, but a small size results in less solution time. Therefore, population size for this case is updated to 80. We concluded that the increase in the HV indicator might be caused by the lack of right tail results of Pareto optimal front.

Table 5.6. Comparison of different number of popSize, case 5U25T

case		*popSize=125*	*popSize=80*
5U25T	***HV indicator***	0.9731	0.9755
	elapsed time(sec)	101.80	62.01

Further, as seen in Table 5.7, average HV indicator value of 5 instances is 0.9672, EA-fUAV results converge to optimal solutions at a rate of around 97%.

Table 5.7. HV indicator values and execution times for the case 5U25T

case		*HV indicator*	*time elapsed (sec)*
	minimum	0.9495	60.76
5U25T	**maximum**	0.9743	63.76
	average	**0.9672**	**61.76**

5.1 Three-Criteria Version of the Problem

In three-criteria version of the problem, the initial step is to find efficient trajectories between pair of targets. This step is accomplished by solving Shortest-Path LP formulation in R, considering all pairs of targets. In three-criteria version of the problem, trajectory selection makes the NP-Hard routing problem more complex and generating the whole Pareto optimal front for the 3-objective cases becomes an infeasible task in an acceptable amount of time. Therefore, we decide to find a subset of optimal solutions which are distributed well enough to represent the nondominated front. In order to get these solutions properly, we need the range of each objective function. These ranges are determined from the payoff table, which is constituted by applying ε-constraint method by considering each criterion in the objective function one by one. Afterwards, these ranges are divided to intervals to get sufficient number of solutions.

For the EA-fUAV, we again run each case for 500 generations and 5 instances are generated for each case with changing initial parents at each instance. Population size is changed regarding the number of UAVs and the targets in the case and mprob is chosen

as 0.6. Then, we analyze the performance of the algorithm for all three cases. We compare the results of EA-fUAV to the optimal results with HV indicator.

3U15T case

Let the total distance traveled by the fleet be the first objective function f_1, total reward collected from targets by the fleet be the second objective function f_2, and total radar threat be the third objective f_3. In the payoff table given in Table 5.8, the minimum and maximum values for the objectives are shown with *. In order to get optimal results to form a representation of the nondominated front, f_1 is specified as the objective, the ranges of f_2 and f_3 are divided to 9 intervals and they are considered as constraints. The models are solved in GAMS using ε-constraint method. In Figure 5.12, optimal results obtained for the three-objective case 4U20T are given.

Table 5.8. Payoff table, case 3U15T

	f_1	f_2	f_3
min f_1	40*	6*	8.54
max f_2	438.98*	80*	42.82*
min f_3	58.74	18	0*

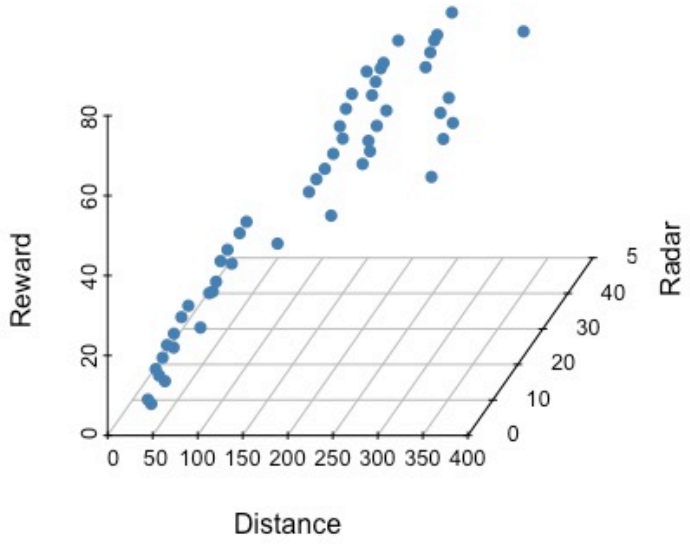

Figure 5.12. Pareto optimal front, case 3U15T, 3 criteria

For the representation of routes on an example, two random nondominated solutions are chosen. In the first solution, a UAV takes off from the base, visits targets 2, 13, 11 in this order and return to the base. Between every pair of targets, the UAV uses first paths; but in the second solution, the UAV changes the path between 11 and 0 and uses the second path. Hence, radar detection threat decreases while distance increases.

In EA-fUAV, crossover probability remains as 0.7 and mutation probability as 0.6. Both optimal and EA-fUAV results are scaled within [0,1] in order to test HV more precisely. 5 different instances are generated to obtain an average test result, which can be seen in Table 5.9. On the average, EA-fUAV results converge to optimal results with approximately 92% rate.

Table 5.9. HV indicator values and execution time for the case 3U15T, 3 criteria

case		***HV indicator***	***time elapsed (sec)***
	minimum	0.8984	209.78
3U15T	**maximum**	0.9360	234.77
	average	**0.9190**	**218.02**

Execution time for finding exact optimal solutions is significantly higher than the execution time of EA-fUAV, the comparison can be seen on Table 5.10.

Table 5.10. Comparison of execution times, case 3U15T, 3 criteria

	time elapsed (sec)	
case	***EA-fUAV***	***optimal***
3U15T	218.02	412344.69

4U20T case

Payoff table for the case 4U20T with 3 criteria is given in Table 5.11. In order to get optimal results to represent the nondominated front, f_1 is specified as the objective, the ranges of f_2 and f_3 (shown with * in the table) are divided to 10 intervals and they are considered as constraints. The models are solved in GAMS using ε-constraint method.

However, because of the excessive run time, execution of method was interrupted. In Figure 5.13, subset of the optimal results generated for the three-objective case 4U20T are given.

Table 5.11. Payoff table, case 4U20T

	f_1	f_2	f_3
min f_1	28.28*	10	0*
max f_2	577.72*	112*	109.25*
min f_3	55.79	3*	0

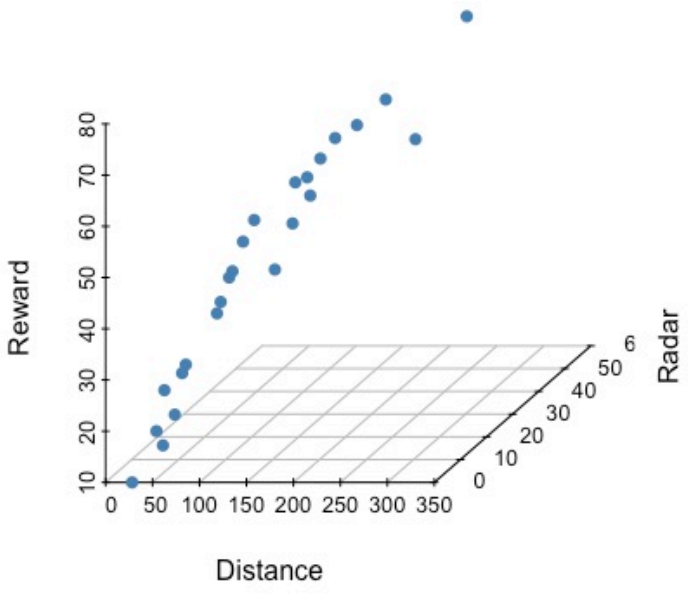

Figure 5.13. Pareto optimal front, case 4U20T, 3 criteria

In order to calculate HV indicator in an accurate way, EA-fUAV results are filtered and the ones with reward higher than the maximum reward of interrupted solutions are eliminated. This procedure is applied to all instances. Then, values are scaled within [0,1] and average HV indicator is calculated as 0.9823, as seen in Table 5.12. We judge that the HV indicator is greater than the 3U15T case because of the set of optimal solutions we could generate. The comparison of execution times would not be fair, since interruption has made but we can still say that EA-fUAV execution time is significantly less than exact method execution time.

Table 5.12. HV indicator values and execution time for the case 4U20T, 3 criteria

case		*HV indicator*	*time elapsed (sec)*
	minimum	0.9631	443.23
4U20T	**maximum**	0.9998	480.81
	average	**0.9823**	**466.94**

5U25T case

Payoff table for the case 5U25T with 3 criteria is given in Table 5.13. In order to get optimal results to form nondominated front, f_1 is specified as the objective, the ranges of f_2 and f_3 (shown by * signs), are divided to 13 intervals, and they are considered as constraints. The models are solved in GAMS using ε-constraint method. However, as in the 4U20T case, because of the excessive run time, execution of method was interrupted. In Figure 5.14, the optimal results generated for the three-objective case 5U25T are given.

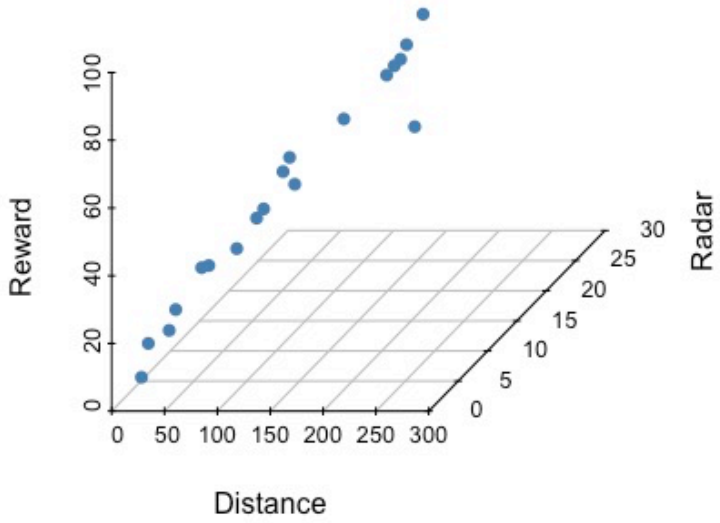

Figure 5.14. Pareto optimal front, case 5U25T, 3 criteria

Table 5.13. Payoff table, case 5U25T

	f_1	f_2	f_3
min f_1	28.28*	10	0*
max f_2	722.03*	137*	105.36*
min f_3	55.79	3*	0

Filtering process for the accurate calculation of HV indicator is done as in the 4U20T case. Average values of 5 different instances are given in Table 5.14, including execution time of EA-fUAV for the case.

Table 5.14. HV indicator values and execution time for the case 5U25T, 3 criteria

case		*HV indicator*	*time elapsed (sec)*
	minimum	0.9495	60.76
5U25T	**maximum**	0.9743	63.76
	average	**0.9672**	**61.76**

As inferred from the results, EA-fUAV converges to the efficient solutions well, with a hypervolume value of at least 90% in each case. Increasing the problem size increases execution time for both solution approaches. When radars are added to the mission area, UAVs also find efficient solutions that avoid passing through the radar regions, increasing the travel distance. Hence, the unvisited number of targets generally increases when three objectives are considered.

6. CONCLUSIONS

In this thesis, we consider the multi-objective routing problem of a fleet of UAVs. The fleet consists of identical UAVs, each having a travel distance limitation due to the fuel capacity and flying with constant speed. There are multiple targets in the mission area, but some of the targets might not be visited as a result of the distance limitations. Different reward values are assigned to the targets; hence we consider maximization of the total reward collected as one of the objectives. Thus, UAVs try to visit as many targets as possible within the travel distance limitation. Since accomplishing the mission in the shortest time has great importance for UAVs employed in defense industry, the second objective of our problem is the minimization of the total distance traveled by the fleet. Moreover, in some mission areas, there are threats like enemy radars for the UAVs and our third objective is to minimize the total radar detection threat. In this thesis, we consider radar-free and radar-monitored terrains separately. In radar-free terrains, we study the first two objectives and find answers to two questions; "Which targets will be visited by which UAV?" and "In which order will these targets be visited?". In terrains monitored with radar, the third objective is added to the study and we also search for an answer to the question: "Which trajectory will be used between two targets?".

The problems are modeled as MOTOP and firstly, we try to find exact optimal solutions with MIP for both versions. In the three-objective version of the problem, initially a MOSPP model is used to determine efficient trajectories between pairs of targets. To address larger problem instances, we propose a heuristic approach which is an EA, a modified version of NSGA-II. We make specific changes in genetic operators of NSGA-II and add repair functions to satisfy the distance limitation in both of the versions.

We test our algorithms on three problem instances, a terrain with 3 UAVs and 15 targets, a terrain with 4 UAVs and 20 targets, and a terrain with 5 UAVs and 25 targets. Our results show that EA-fUAV approximates the Pareto-optimal frontier well in all instances. Specifically, both in two and three criteria versions and in all three cases of the problem, EA-fUAV results approximate at least 90% of the Pareto front. As the problem gets larger, the exact solution run times increase substantially, but the EA-fUAV run times

change reasonably. This reinforces the preferability of EA-fUAV since it can be readily used in practice. It can also be used for different vehicle routing applications.

The main limitation of the computational study was the excessive run times of the mathematical models for the problem. Also, we needed to generate the problem instances manually, to test the algorithms on problems that are as realistic as possible. Further research on routing a fleet of UAVs can be extending the results to a 3-dimensional area including geographical conditions and constraints. Also, the decision maker's preferences can be incorporated in the solution process. Besides, target and radar locations may be considered as dynamic in future studies.

In conclusion, we considered the UAV routing problem in both radar-free and radar-monitored terrains as MOTOP. To the best of our knowledge, all three objectives are not considered in any study in the literature that routes a fleet of UAVs. We developed solution approaches for both versions. Our computational results show that, our algorithm EA-fUAV runs in short times and approximates the efficient solutions well.

REFERENCES

Alotaibi, K.A., Rosenberger, J.M., Mattingly, S.P., Punugu, R.K., Visoldilokpun, S., Unmanned aerial vehicle routing in the presence of threats, Comput. Ind. Eng., 115 (**2018**) 190–205.

Austin, R., Unmanned Air Systems: UAV Design, Development and Deployment, Wiley, **2010**.

Chankong, V., Haimes, Y.Y., Multiobjective Decision Making: Theory and Methodology, North-Holland, New York, **1983**.

Chao, I.-M., Golden, B.L., Wasil, E.A., The team orienteering problem, Eur. J. Oper. Res., (**1996**) 464–474.

Coutinho, W.P., Battarra, M., Fliege, J., Computers & Industrial Engineering The unmanned aerial vehicle routing and trajectory optimisation problem, a taxonomic review, Comput. Ind. Eng., 120 (**2018**) 116–128.

Deb, K., Multi-Objective Optimization Using Evolutionary Algorithms, Wiley, **2001**.

Deb, K., Member, A., Pratap, A., Agarwal, S., Meyarivan, T., A Fast and Elitist Multiobjective Genetic Algorithm : NSGA-II. IEEE Trans. Evol. Comput., 6 (**2002**) 182–197.

Gudaitis, M.S., Multicriteria Mission Route Planning Using a Parallel A* Search, M.S. Thesis, Air Force Institute of Technology, **1994**.

Hernández-Hernández, L., Tsourdos, A., Shin, H.-S., Waldock, A., Multi-objective UAV routing, in: International Conference on Unmanned Aircraft Systems (ICUAS), **2014**, p. 534–542.

Karakaya, M., UAV Route Planning for Maximum Target Coverage, Comput. Sci. Eng. An Int. J., 4 (**2014**) 27–34.

Korkmaz, Y., İyibilgin, O., Fındık, F., Geçmişten günümüze insansız hava araçlarının gelişimi, SAÜ Fen Bilim. Enstitüsü Derg. 20 (**2015**) 103.

Köksalan, M., Tezcaner Öztürk, D., An evolutionary approach to generalized biobjective traveling salesperson problem, Comput. Oper. Res. 79 (**2017**) 304–313.

Lamont, G.B., Slear, J.N., Melendez, K., UAV Swarm Mission Planning and Routing using Multi-Objective Evolutionary Algorithms, in: IEEE Sympoisum on Computational Intelligence in Multicriteria Decision Making, **2007**, p. 10–20.

Levy, D., Sundar, K., Rathinam, S., Heuristics for Routing Heterogeneous Unmanned Vehicles with Fuel Constraints, Math. Probl. Eng, **2014**.

Mavrotas, G., Effective implementation of the e-constraint method in Multi-Objective Mathematical Programming problems, Appl. Math. Comput. 213 (**2009**) 455–465.

Ousingsawat, J., UAV Path Planning for Maximum Coverage Surveillance of Area with Different Priorities, in: The 20th Conference of Mechanical Engineering Network of Thailand, **2006**.

Peng, X., Gao, X., A Multi-objective Optimal Approach for UAV Routing in Reconnaissance Mission with Stochastic Observation Time, in: Foundations of Intelligent Systems, ISMIS 2008, **2008**, p. 246–255.

Sundar, K., Rathinam, S., Algorithms for Routing an Unmanned Aerial Vehicle in the Presence of Refueling Depots, IEEE Trans. Autom. Sci. Eng., 11 (**2014**) 287–294.

Tezcaner, D., Köksalan, M., An Interactive Algorithm for Multi-objective Route Planning, J. Optim. Theory Appl., 150 (**2011**) 379–394.

Tezcaner Öztürk, D., Heuristic and Exact Approaches for Multi-Objective Routing, PhD Thesis, The Graduate School of Natural and Applied Sciences of Middle East Technical University, Ankara, **2013**.

Tezcaner Öztürk, D., Köksalan, M., Biobjective UAV route planning in Continuous Terrain, Technical Report, Department of Industrial Engineering, METU, **2018**.

Tezcaner Öztürk, D., Köksalan, M., An interactive approach for biobjective integer programs under quasiconvex preference functions, Ann. Oper. Res., 244 (**2016**) 677–696.

Türeci, H., Interactive Approaches for Bi-Objective UAV Route Planning in Continuous Space, M.S. Thesis, The Graduate School of Natural and Applied Sciences of Middle East Technical University, Ankara, **2017**.

Valavanis, K.P., Vachtsevanos, G.J., Handbook of Unmanned Aerial Vehicles, Springer Reference, **2015**.

Van Veldhuizen, D.A., Multiobjective Evolutionary Algorithms: Classifications, Analyses, and New Innovations, PhD Thesis, Air Force Institute of Technology, **1999**.

Winston, W.L., Operations Research, Applications and Algorithms, 4th ed, Thomson Learning, **2004**.

Wu, W., Wang, X., Cui, N., Fast and coupled solution for cooperative mission planning of multiple heterogeneous unmanned aerial vehicles, Aerosp. Sci. Technol., 79 (**2018**) 131–144.

Yakıcı, E., Solving location and routing problem for UAVs, Comput. Ind. Eng., 102 (**2016**) 294–301.

Zitzler, E., Thiele, L., Multiobjective Evolutionary Algorithms : A Comparative Case Study and the Strength Pareto Approach, IEEE Trans. Evol. Comput., 3 (**1999**) 257–271.

APPENDIX

Appendix-1 – Continuous mission area, case 4U20T

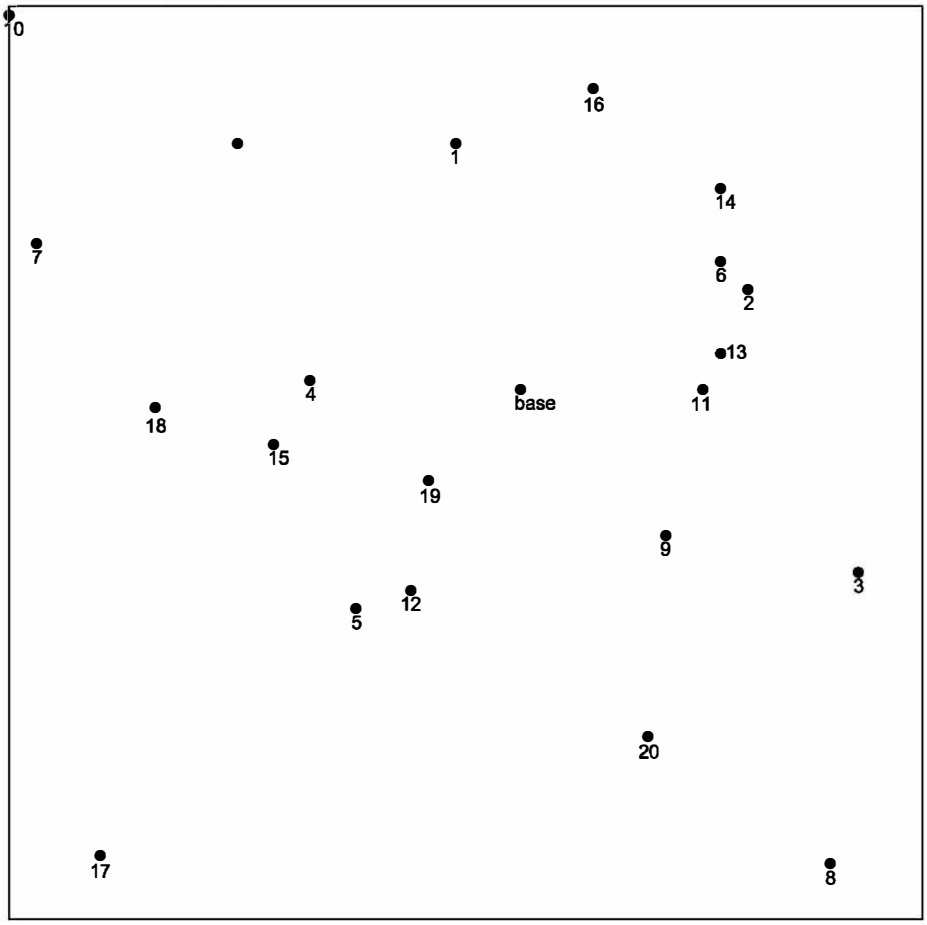

Figure 1. Continuous mission area, case 4U20T

Appendix-2 – Continuous mission area, case 5U25T

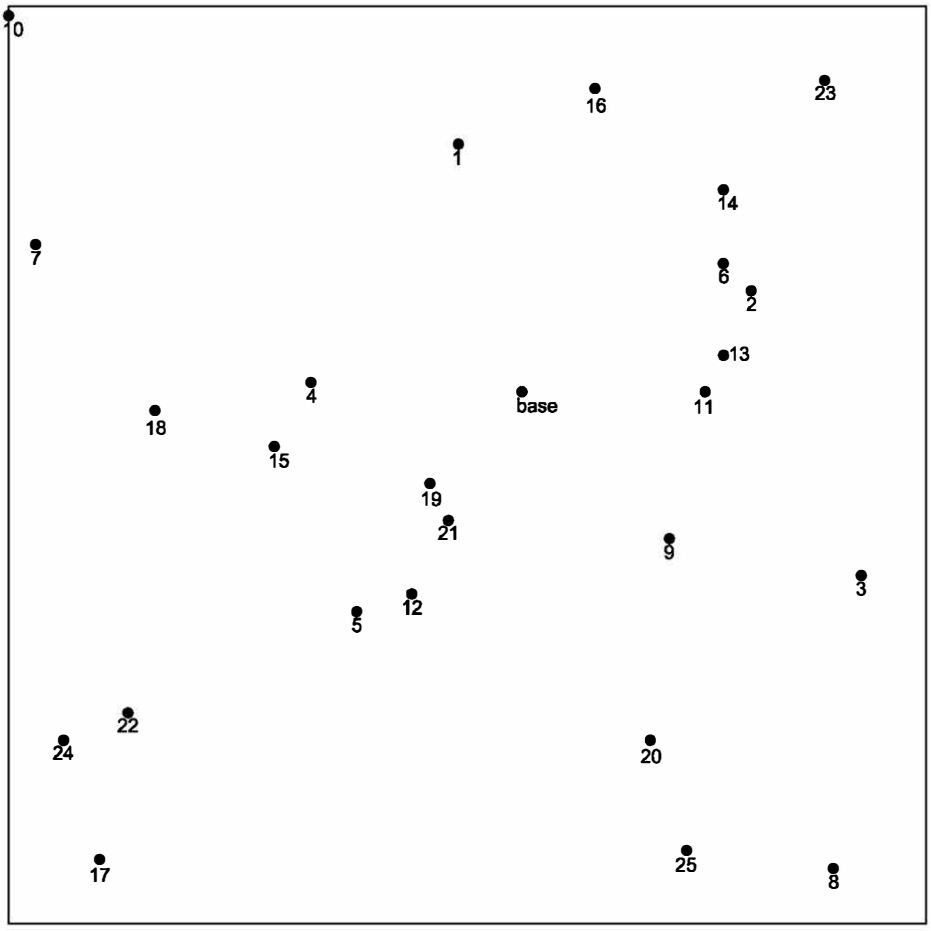

Figure 2. Continuous mission area, case 5U25T

Appendix-3 – Mission area with radar, case 4U20T

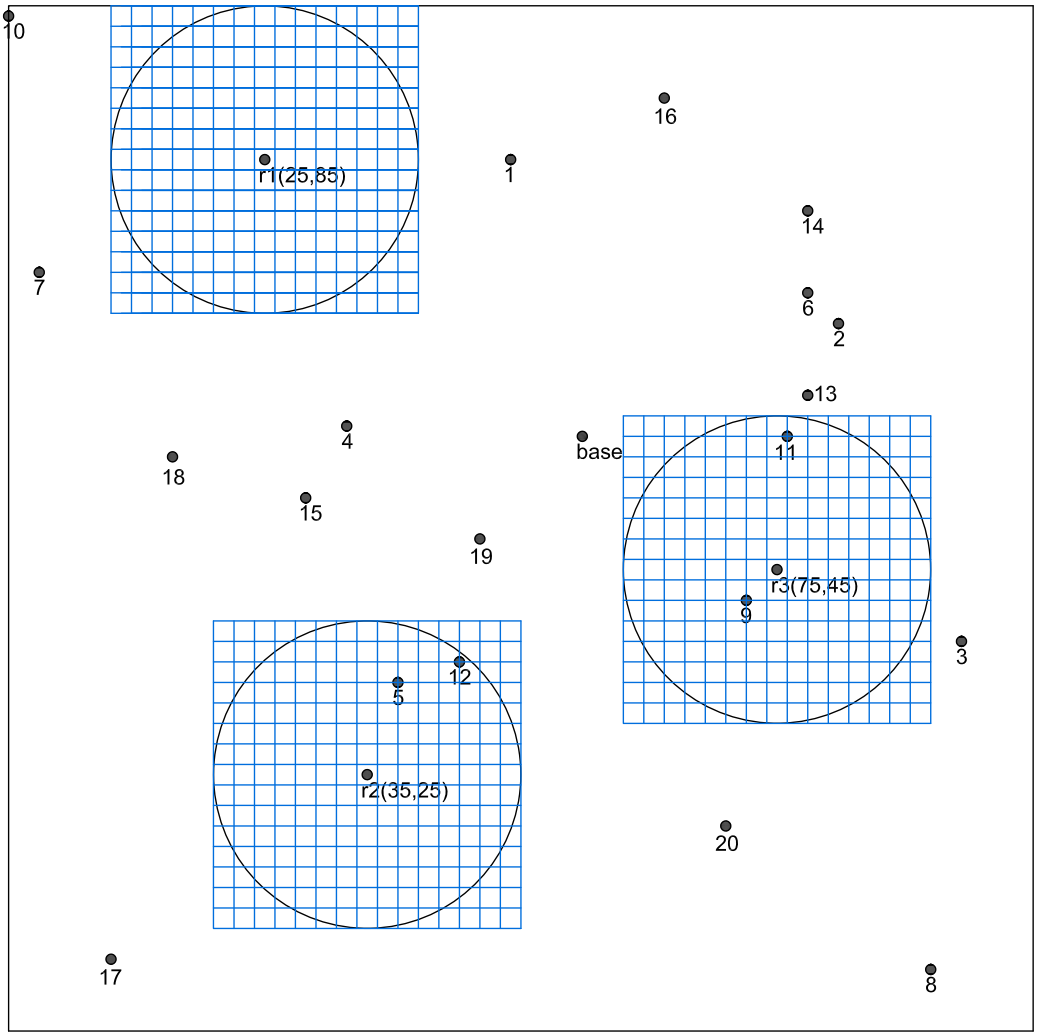

Figure 3. Mission area with radar, case 4U20T

Appendix-4 – Mission area with radar, case 5U25T

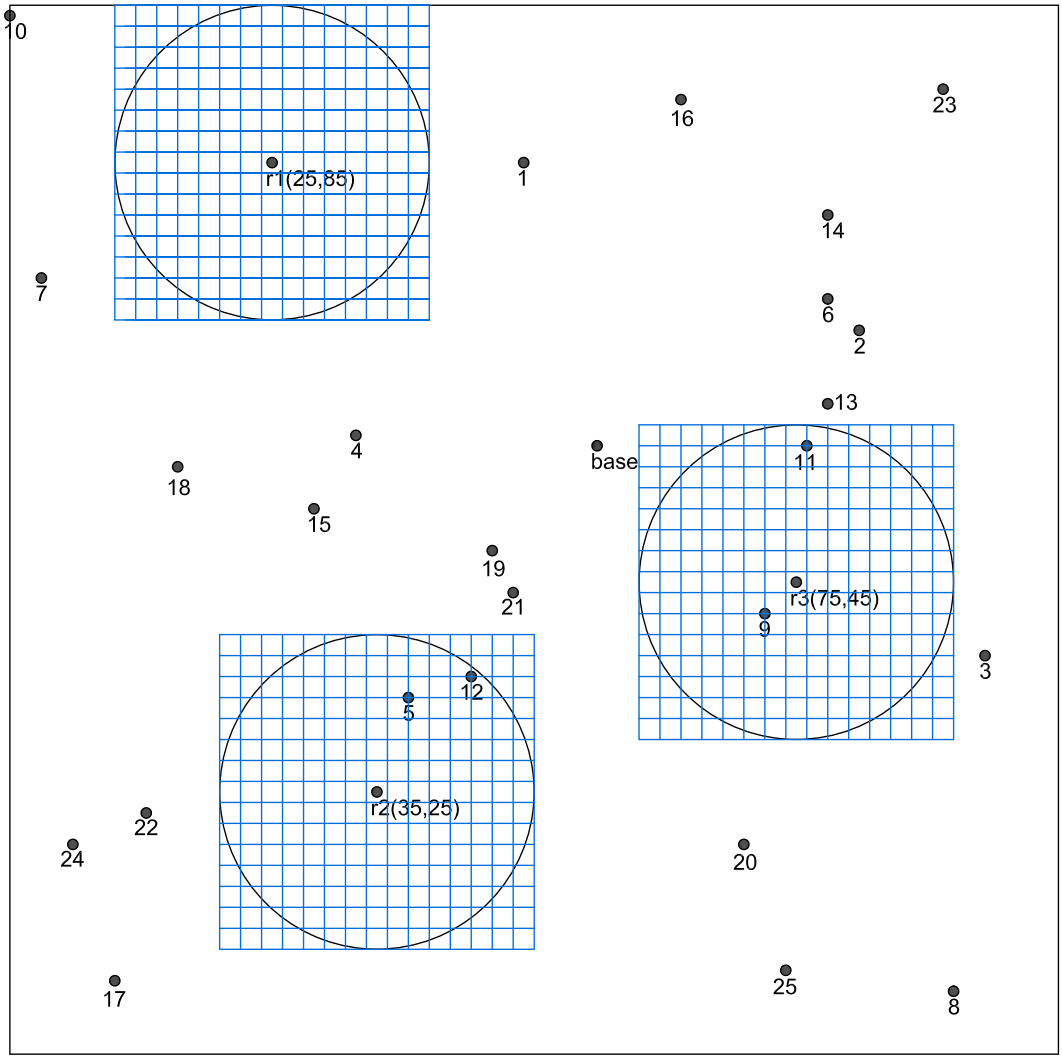

Figure 4. Mission area with radar, case 5U25T